RSC Advances

PAPER

View Article Online
View Journal | View Issue



Cite this: *RSC Adv.*, 2018, **8**, 11871

# SAR study on $N^2$,$N^4$-disubstituted pyrimidine-2,4-diamines as effective CDK2/CDK9 inhibitors and antiproliferative agents†

Liandong Jing,[a] Yanbo Tang,[a] Masuo Goto,[b] Kuo-Hsiung Lee[bc] and Zhiyan Xiao*[a]

Received 14th February 2018
Accepted 21st March 2018

DOI: 10.1039/c8ra01440j

rsc.li/rsc-advances

Cyclin-dependent kinases (CDKs) are pivotal kinases in cell cycle transition and gene transcription. A series of $N^2$,$N^4$-diphenylpyrimidine-2,4-diamines were previously identified as potent CDK2/CDK9 inhibitors. To explore the SAR of this structural prototype, twenty-four novel $N^2$,$N^4$-disubstituted pyrimidine-2,4-diamines were designed and synthesized. Among them, twenty-one compounds exhibited potent inhibitory activities against both CDK2/cyclin A and CDK9/cyclin T1 systems, and the most potent CDK2 and CDK9 inhibitors, **3g** and **3c**, showed $IC_{50}$ values of 83 nM and 65 nM respectively. Most of these compounds displayed significant inhibition against the tested tumor cell lines in the SRB assay, and in particular, remained active against the triple-negative breast cancer (TNBC) cell line MDA-MB-231. Flow cytometer analysis of compounds **2a**, **2d** and **3b** in MDA-MB-231 cells indicated that these compounds induced cell cycle arrest in G2/M phase. Docking studies on compound **3g** were performed, which provided conducive clues for further molecular optimization.

## Introduction

Cyclin-dependent kinases (CDKs) are a family of serine–threonine protein kinases. Upon binding to their regulatory partner cyclins, CDKs can be activated and play critical roles in cell cycle transition and gene transcription. Up to now, 20 CDKs and 29 cyclins have been identified from the human proteome. These CDKs and cyclins form a myriad of different heterodimeric complexes and modulate a variety of physiological and pathological processes.[1,2] As a representative member in cell-cycle regulation, CDK2 plays a key role in the control of G1-S phase transition when in complex with cyclin E, while CDK2–cyclin A complex is required for the transition of the S phase.[3,4] Different from CDK2, the transcriptional CDK9 appears to have a minimal effect on cell cycle transition.[5] In contrast, CDK9/cyclin T is involved in the regulation of RNA transcription as the catalytic subunit of positive transcription elongation factor (P-TEFb).[6,7]

The recognition of the pivotal roles of CDKs has stimulated extensive research interests on CDK inhibitors in recent two decades.[8,9] A number of structural diverse CDK inhibitors are currently under active clinical investigations for the treatment of cancer (Fig. 1A),[10,11] and four inhibitors have received approval from the U. S. Food and Drug Administration (FDA) (Fig. 1B). Flavopiridol (alvocidib) is the first CDK inhibitor approved by FDA. As a pan-CDK inhibitor competing with ATP, alvocidib was granted an orphan drug designation in the E. U. for the treatment of chronic lymphocytic leukemia (CLL) in 2007.[12] It was later approved for the treatment of acute myeloid leukemia (AML) in both the US and the EU.[12] The advent of selective CDK4/6 inhibitors symbolizes an important breakthrough in the translational research of CDK inhibitors,[13,14] and has led to the successive approvals of palbociclib from Pfizer, ribociclib from Novartis and abemaciclib from Eli Lilly by the FDA in the recent three years.[12] These therapeutic drugs selectively target the cyclin D-CDK4/6 axis and have made significant contributions to the treatment of hormone receptor (HR)-positive, human epidermal growth factor receptor 2 (HER2)-negative breast cancer.

As representative cell cycle regulatory CDK and transcriptional CDK, CDK2 and CDK9 have been widely investigated for their potent inhibitors. In our previous efforts, a 3D-QSAR pharmacophore derived from a diverse set of known CDK9 inhibitors was constructed.[15] Guided by the pharmacophoric features revealed and structural requirements of the ATP sites of CDK2 and CDK9, a series of novel $N^2$,$N^4$-diphenylpyrimidine-2,4-diamines were designed and

[a]*Beijing Key Laboratory of Active Substance Discovery and Druggability Evaluation, Institute of Materia Medica, Chinese Academy of Medical Sciences, Peking Union Medical College, Beijing 100050, China. Tel: +86-10- 63189228. E-mail: xiaoz@imm.ac.cn*

[b]*Natural Products Research Laboratories, UNC Eshelman School of Pharmacy, University of North Carolina, Chapel Hill, North Carolina 27599-7568, USA*

[c]*Chinese Medicine Research and Development Center, China Medical University and Hospital, Taichung, Taiwan*

† Electronic supplementary information (ESI) available. See DOI: 10.1039/c8ra01440j

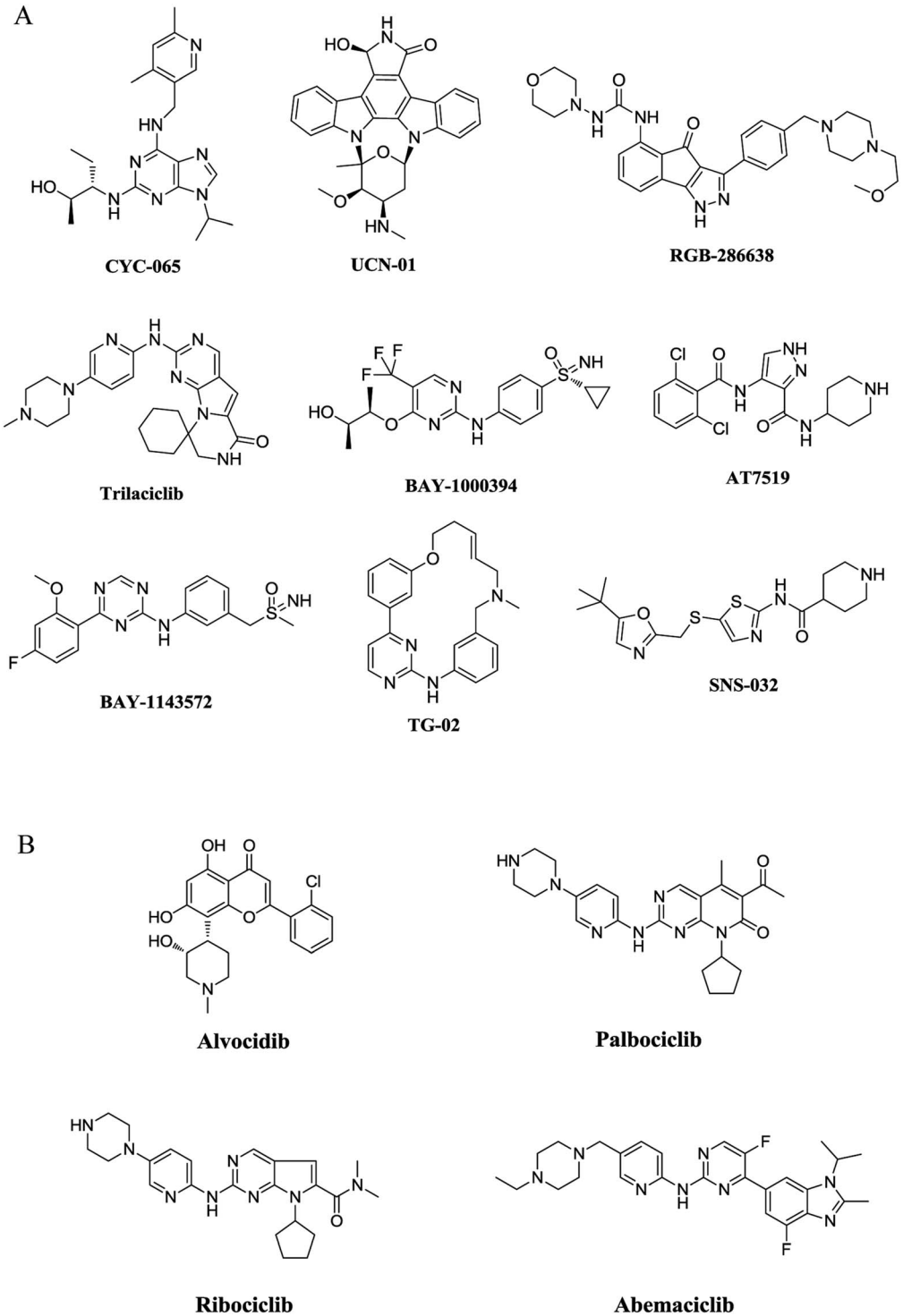


Fig. 1 Representative structures of CDK inhibitors. (A) Representative structures of CDK inhibitors in clinical trials. (B) Structures of CDK inhibitors approved by FDA.

synthesized, and compound **1** (Fig. 2) was identified as the most potent inhibitor against CDK2 and CDK9.[16] We report herein the exploration of structure–activity relationships (SAR) on compound **1**. Accordingly, twenty-four novel $N^2$,$N^4$-disubstituted pyrimidine-2,4-diamines were prepared and evaluated.

## Results and discussion

### Molecular design

As illustrated in Fig. 2, a stepwise molecular optimization was applied to the scaffold of compound **1**, and the molecular areas A, B, C and D in **1** were modified to explore SAR. For area A,

 

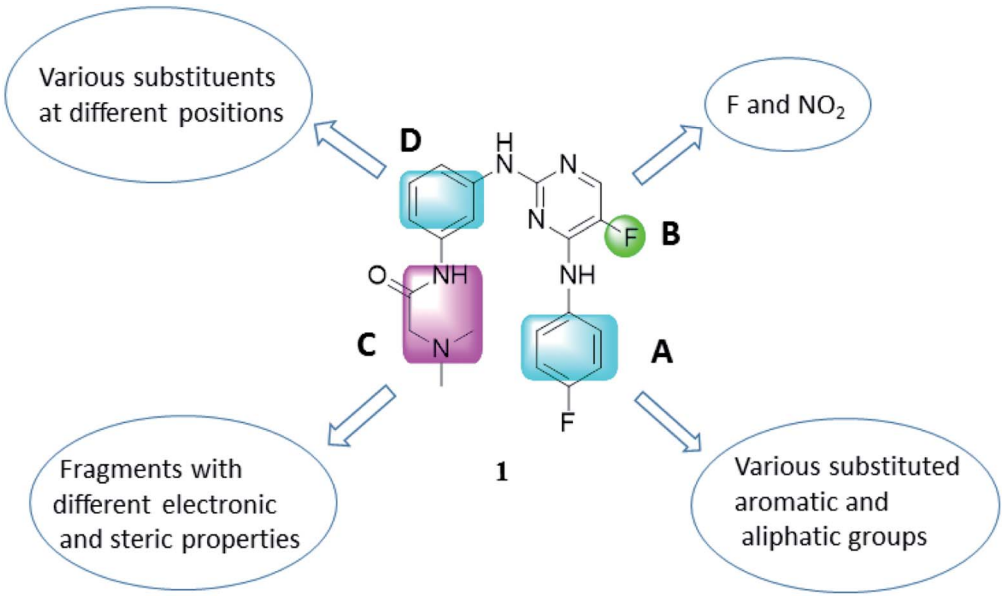


Fig. 2 Molecular optimization based on compound 1.

various substituted aromatic and aliphatic groups were introduced to investigate their effects on kinase inhibitory activity (Table 1, **2a–2h**). It was also attempted to replace the fluoro atom in area B by nitro group (Table 1, **2i**). Previous molecular docking suggested a change of Lys89 (CDK2) to Gly122 (CDK9) in the sub-pocket occupied by the *N*,*N*-dimethyl glycine moiety in area C.[16] This observation implied that CDK2/CDK9 selectivity might be sensitive to the size and charge status in this molecular area. Therefore, various fragments with different electric and steric properties were extracted from known CDK inhibitors and grafted to area C (Table 2, **3a–3e**, **3m–3o**).[17] Various substituents were also introduced at different positions of the benzene ring in area D (Table 2, **3f–3l**). Such molecular optimization was expected to provide preliminary SAR on the prototype structure of **1**. For all the molecular areas, electrophilic moieties were avoided intently to maintain the reversible nature of the inhibitors.

## Chemistry

The general synthetic route for compounds **2a–2i** was shown in Scheme 1. The key intermediate **6** was produced from the starting material **4** by reacting with *N*,*N*-dimethylglycine hydrochloride in the presence of 2-(1*H*-7-azabenzotriazol-1-yl)-1,1,3,3-tetramethyl-uronium hexafluorophosphate (HATU) and *N*,*N*-diisopropylethylamine (DIEA), and catalytic hydrogenation by Pd/C. The other key intermediate **8** was prepared by regioselective substitution of compound **7** with appropriate amines.[16] Cross-coupling between **6** and **8** under microwave irradiation afforded the target compounds **2a–2i**.

The synthetic routes to compounds **3a–3l** are illustrated in Scheme 2. The intermediates **9**, **11** and **13** were prepared through a C–N cross-coupling reaction between **8e** and appropriate amines. Catalytic hydrogenation of compounds **9** and **11** was performed to afford compounds **10** and **12**. The target compounds **3a–3l** were synthesized by condensation between appropriate amines and acids in the presence of HATU and DIEA.

The synthesis of compounds **3m–3o** is outlined in Scheme 3. The intermediate **16** was prepared through successive cross-coupling and catalytic hydrogenation, which was subsequently subjected to C–N cross-coupling to provide compounds **3m–3o**.

## CDK2/cyclin A and CDK9/cyclin T1 inhibition

All the target compounds were initially tested against CDK2/cyclin A and CDK9/cyclin T1. The inhibitory activities of these compounds in terms of $IC_{50}$ values were shown in Tables 1 and 2. Most of the compounds showed significant inhibition against both CDK2/cyclin A and CDK9/cyclin T1 systems, and were more potent than the prototype structure **1**. As demonstrated in Table 1, various substituents on the phenyl ring in $R^1$ were generally well accommodated (**2a–2g** *vs.* **1**), whereas the variation in substitution patterns (*e.g.* type, position and number of substituents) did lead to a slight fluctuation in the inhibitory activity (**2a** *vs.* **1**, **2e** *vs.* **2g**, **2e** *vs.* **1**). Among the substitution patterns investigated, 2,6-difluorophenyl (**2e**) seemed to be optimal for $R^1$, and compound **2e** exhibited $IC_{50}$ values of 0.24 μM and 0.095 μM against CDK2/cyclin A and CDK9/cyclin T1, respectively. However, the introduction of aliphatic fragment 4-methylpiperazin-1-yl at $R^1$ caused a moderate decrease in the inhibitory activity (**2h** *vs.* **1**). Decreased inhibition was also observed when the fluoro atom in area B was replaced by nitro group (**2e** *vs.* **2i**).

For compounds in Table 2, the optimal 2,6-difluorophenyl substitution at $R^1$ (**2e**) was preserved, and SAR exploration in area D, in particular the substitution patterns of the phenyl ring, was performed. At a first glance of data in Table 2, it is surprising to find that the tolerance for substitution at $R^3$ (C-2′ of the phenyl) was rather poor, and any substituent other than

Table 1 Inhibitory effects of compounds **2a–2i** against CDK2/cyclin A and CDK9/cyclin T1

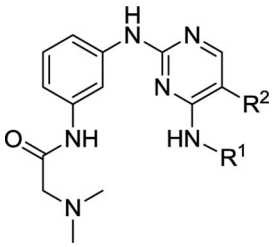

| Compd. | $R^1$ | $R^2$ | $IC_{50}$[a] (μM) CDK2/cyclin A | $IC_{50}$[a] (μM) CDK9/cyclin T1 |
|---|---|---|---|---|
| **1** | 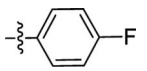 | F | 1.71 | 0.78[b] |
| **2a** | 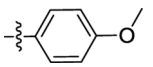 | F | 0.32 ± 0.28 | 0.30 ± 0.01 |
| **2b** | 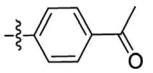 | F | 0.78 ± 0.04 | 0.39 ± 0.08 |
| **2c** | 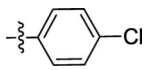 | F | 0.91 ± 0.11 | 1.10 ± 0.02 |
| **2d** | 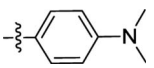 | F | 0.94 ± 0.43 | 0.32 ± 0.05 |
| **2e** | 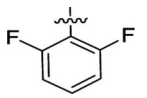 | F | 0.24 ± 0.04 | 0.095 ± 0.004 |
| **2f** | 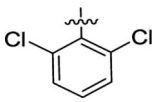 | F | 1.60 ± 0.11 | 0.57 ± 0.12 |
| **2g** | 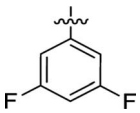 | F | 0.57 ± 0.05 | 0.49 ± 0.27 |
| **2h** | 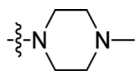 | F | 5.60 ± 0.53 | 2.20 ± 0.32 |
| **2i** | 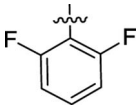 | $NO_2$ | 0.78 ± 0.12 | 0.48 ± 0.08 |

[a] The $IC_{50}$ value was interpolated from dose–response data with six different concentrations. Each test was performed in duplicate. Data represent the average of duplicate measurements. [b] The data were cited from ref. 16.

a hydrogen atom might result in dramatic loss of inhibitory activity (**3f** *vs.* **1** and **3g**, **3h** *vs.* **3i**, **3k** *vs.* **3l**). This is probably due to an interference posed by the substituent to the key hydrogen bonding interaction between the N-1 atom/2-amino and the hinge region of the kinase. In contrast, substitution at $R^4$ showed no significant effects on the inhibitory activity (**2e** *vs.* **3i** and **3j**), and the exchange of substituents at $R^3$ and $R^4$ had little influence on kinase inhibition (**2e** *vs.* **3k**). As expected, a range of substituents with different electronic and steric properties, which were extracted from known CDK inhibitors, were generally well accepted at $R^5$ of the C5′ position (**3a–3e**, **3m**, **3n** *vs.* **2e**, **3j** *vs.* **3o**). Interestingly, the incorporation of a methyl at $R^4$ in **3j** resulted in moderate subtype selectivity (about 18-fold for CDK9 over CDK2), which implied that modification at $R^4$ might be an attemptable approach to achieve subtype selectivity. It was previously suggested that the orientation of the morpholino ring at $R^5$ might be responsible for the selectivity to CDK9 over CDK2.[16] Methyl was introduced at $R^4$ intently (**3o**), and it is assumed to affect the orientation of the morpholino ring at $R^5$ so as to alter the subtype selectivity. However, compound **3o** displayed only 7.5-fold selectivity towards CDK9, which is less selective than its congener without methyl substitution. The biological data listed in Tables 1 and 2 revealed obvious SAR trends for this compound class, and such results implied specific inhibition against the targets.

### Inhibitory activities against tumor cell lines

All the compounds that showed significant inhibition in the enzymatic assays were further tested against the tumor cell lines, including MDA-MB-231, MCF-7, A549, KB and KB-vin in the sulforhodamine B (SRB) assay. The inhibitory activities of the target compounds in terms of $GI_{50}$ values were demonstrated in Table 3. Most of the tested compounds displayed potent antiproliferative activities against the five human tumor cell lines and showed $GI_{50}$ values at micromolar or even submicromolar level. Nevertheless, there was no obvious correlation between molecular enzymatic inhibition and cellular cytotoxicity, which might mainly owe to the variation in cellular concentration caused by different physicochemical properties. Notably, these compounds were not only active against the vincristine-resistant cell line KB-vin, but also the triple-negative breast cancer (TNBC) cells MDA-MB-231, which is a clinically aggressive form generally unresponsive to chemotherapy.

### Effects on cell cycle progression in MDA-MB-231 cells

To evaluate their effects on the cell cycle progression, compounds **2a**, **2d** and **3b**, which were the most potent compounds against MDA-MB-231 cells, were subjected to flow cytometry following protocols described previously.[18] As depicted in Fig. 3, compounds **2a**, **2d** and **3b** imposed obvious effects on the cell cycle progression under a concentration of five-fold $IC_{50}$. It seemed that these compounds inhibited the onset of mitosis and induced cell cycle arrest at G2/M. Such observations implied that they might target proteins critical for the onset of mitosis. While CDK2 is generally regarded as a G1/S and S phase regulator, cell cycle arrest at the G2/M has been previously reported for CDK1 inhibition.[19] This observation, in combination with the comparable inhibitory activities against both CDK2 and CDK9 systems for these compounds suggested that these compounds were likely to be pan-CDK inhibitors and multiple CDKs could be involved in the cells growth inhibition induced by compounds **2** and **3**. In addition, as a privileged scaffold for kinase inhibitors, the pyrimidine scaffold were also found in

 

Table 2 Inhibitory effects of compounds **3a–3o** against CDK2/cyclin A and CDK9/cyclin T1

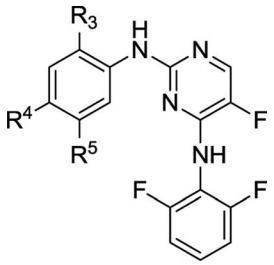


| Compd. | $R^3$ | $R^4$ | $R^5$ | $IC_{50}$[a] (μM) CDK2/cyclin A | CDK9/cyclin T1 |
|---|---|---|---|---|---|
| **2e** | H | H | 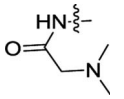 | 0.24 ± 0.04 | 0.095 ± 0.004 |
| **3a** | H | H | 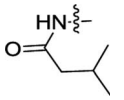 | 1.10 ± 0.15 | 0.48 ± 0.22 |
| **3b** | H | H | 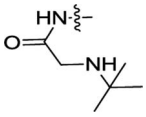 | 0.38 ± 0.06 | 0.08 ± 0.001 |
| **3c** | H | H | 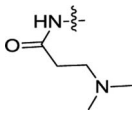 | 0.30 ± 0.07 | 0.065 ± 0.023 |
| **3d** | H | H | 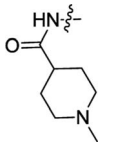 | 0.13 ± 0.02 | 0.66 ± 0.02 |
| **3e** | H | H | 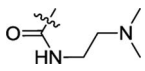 | 0.75 ± 0.14 | 0.23 ± 0.01 |
| **3f** | F | H | 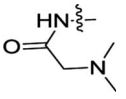 | ND[b] | ND |
| **3g** | H | F | 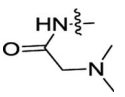 | 0.083 ± 0.035 | 0.10 ± 0.01 |
| **3h** | $OCH_3$ | H | 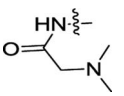 | ND | ND |
| **3i** | H | $OCH_3$ | 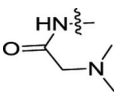 | 0.57 ± 0.08 | 0.19 ± 0.02 |
| **3j** | H | $CH_3$ | 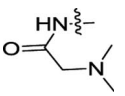 | 2.90 ± 0.06 | 0.16 ± 0.02 |
| **3k** | H | 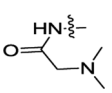 | H | 0.44 ± 0.04 | 0.083 ± 0.002 |

Table 2 (*Contd.*)

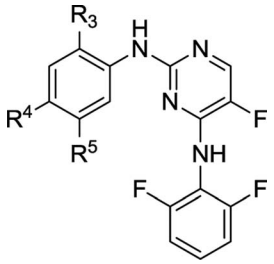

| Compd. | $R^3$ | $R^4$ | $R^5$ | $IC_{50}$[a] (μM) CDK2/cyclin A | $IC_{50}$[a] (μM) CDK9/cyclin T1 |
|---|---|---|---|---|---|
| **3l** | 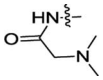 | H | H | ND | ND |
| **3m** | H | H | 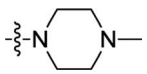 | 0.47 ± 0.04 | 0.290 ± 0.002 |
| **3n** | H | H | 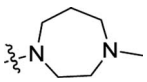 | 0.95 ± 0.27 | 1.6 ± 0.1 |
| **3o** | H | $CH_3$ | 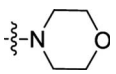 | 5.60 ± 0.03 | 0.74 ± 0.04 |

[a] The $IC_{50}$ value was interpolated from dose–response data with six different concentrations. Each test was performed in duplicate. Data represent the average of duplicate measurements. [b] Not determined due to the lack of significant inhibition at the concentration of 10 μM.

inhibitors against other kinases, such as aurora, ALK, PI3K.[20–22] Taking together, these inhibitors were likely to exert inhibitory effects against tumor cells *via* non-selective inhibition against multiple CDKs and even members of other kinase families.

### Molecular modeling

Due to the structural similarity between compound **3g** and the inhibitor co-crystalized, the 3D structures of 4BCP (CDK2) and 4BCG (CDK9) were selected for docking studies on compound **3g** to explore its interaction modes with both CDK2 and CDK9 (Fig. 4). As illustrated by Fig. 4A, compound **3g** situated in the ATP-binding site of CDK9, where the *N*,*N*-dimethyl glycine moiety occupied the outside sub-pocket, and the N-1 atom as well as 2-amino moiety on the pyrimidine ring interacts with the hinge residue Cys106 through hydrogen bonding. The 2,6-difluorophenyl moiety protruded toward the inside sub-pocket, and π–π stacking interactions were monitored between 2,6-difluorophenyl and Phe103, as well as between the pyrimidine ring and Phe105. Besides, hydrophobic interactions between **3g** and residues Ala46 and Leu156 were detected in the binding pocket. As depicted by Fig. 4B, **3g** adopted a similar pose in the ATP-binding site of CDK2. The *N*,*N*-dimethyl glycine moiety occupied the outside pocket and 2,6-difluorophenyl moiety situated inside. Hydrogen bonding was also observed between N-1 atom/2-amino moiety of **3g** and the hinge residue Leu83. Besides, hydrophobic interactions between **3g** and residues Val18, Ala31 and Leu134 were detected in CDK2. The insights gained from docking studies might guide further molecular design of potent CDK inhibitors. Whereas, the almost identical interaction modes of compound **3g** with either CDK9 or CDK2 implied severe challenges to achieve subtype selectivity.

## Experimental

### Chemistry

Chemical reagents and solvents were obtained from commercial sources and were used without further purification. When necessary, solvents were dried and/or purified by standard methods. All reactions were monitored by thin-layer chromatography with preparative silica gel F254 plates purchased from Merck, Inc. Flash chromatography was performed using either a glass column packed with silica gel (200–300 mesh) or pre-packed silica gel cartridges by a combi-flash machine from Teledyne Isco. The purity of all target compounds assayed was identified by thin-layer chromatography (silica gel F254) and NMR spectra. In particular, the purity of the most active compounds, **2a**, **2d** and **3b**, was further determined by HPLC (ESI†). $^1$H-NMR spectra were recorded on Varian Mercury 300 MHz or 400 MHz spectrometer. $^{13}$C-NMR spectra were recorded on Varian Mercury 400 MHz or 500 MHz spectrometer. Chemical shifts are reported in parts per million ($\delta$) relative to internal

 

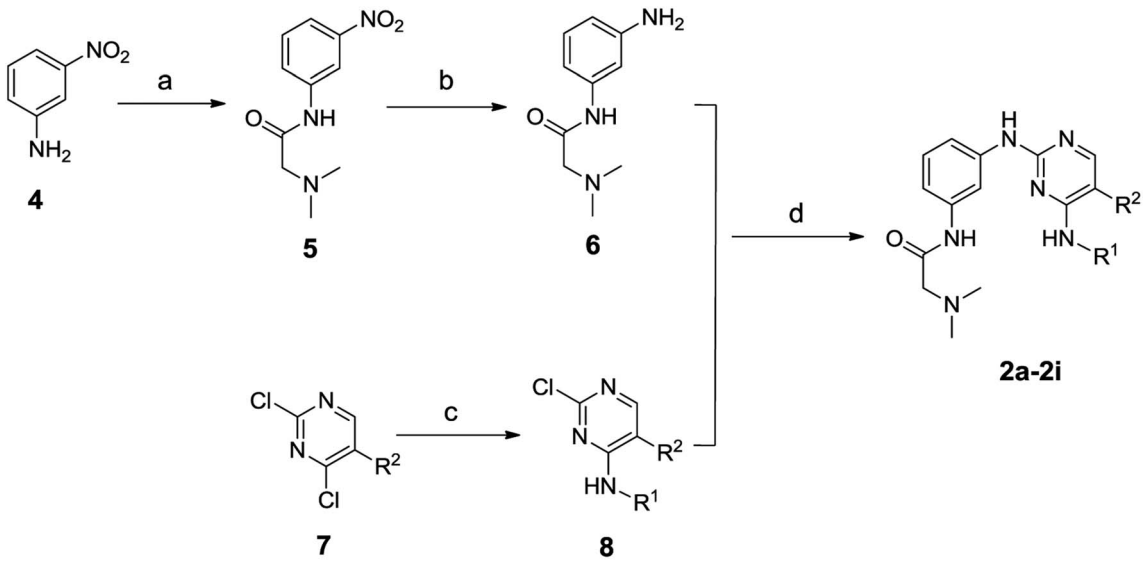


**2a:** $R^1$= 4-OMe-phenyl, $R^2$ = F
**2b:** $R^1$= 4-acetyl-phenyl, $R^2$ = F
**2c:** $R^1$= 4-Cl-phenyl, $R^2$ = F
**2d:** $R^1$= 4-$(CH_3)_2$-N-phenyl, $R^2$ = F
**2e:** $R^1$= 2,6-di-F-phenyl, $R^2$ = F
**2f:** $R^1$= 2,6-di-Cl-phenyl, $R^2$ = F
**2g:** $R^1$= 3,5-di-F-phenyl, $R^2$ = F
**2h:** $R^1$= 4-*N*-methyl-piperazinyl, $R^2$ = F
**2i:** $R^1$= 2,6-di-F-phenyl, $R^2$ = $NO_2$

Scheme 1 Synthesis of compounds **2a–2i**. *Reagents and conditions: (a) *N*,*N*-dimethylglycine hydrochloride, HATU, DIEA, dichloromethane, 63%; (b) Pd/C, $H_2$, $CH_3OH$/ethyl acetate, 95%; (c) appropriate amine, MeOH/$H_2O$, 35%; or $Et_3N$/EtOH, 48–74%; (d) $Pd(OAc)_2$, xantphos, $Cs_2CO_3$, dry THF, $N_2$, microwave irradiation, 20–57%.

tetramethylsilane (TMS) standard. Coupling constants are given in hertz. All melting points were determined on Yanaco melting point apparatus. Mass spectra were taken in HR-ESI mode on Exactive Plus™ LC/MSD Orbitrap from Thermo Fisher Scientific. Reactions under microwave irradiation were performed in a Biotage Initiator microwave reactor in sealed vessels.

### Preparation of 3-(dimethylamino-acetamino) aniline (6)

3-Nitroaniline **4** (276 mg, 2 mmol) and *N*,*N*-dimethylglycine hydrochloride (419 mg, 3 mmol) were dissolved in $CH_2Cl_2$. HATU (1.14 g, 3 mmol) and DIEA (1.29 g, 10 mmol) were then added. The reaction mixture was stirred at room temperature overnight. After the solvent was evaporated, the residue was dissolved in ethyl acetate and then washed with saturated sodium bicarbonate solution. The organic layer was concentrated and the crude material was purified by column chromatography on silica gel, eluted with petroleum ether/ethyl acetate (20 : 1) to afford compound **5** as a yellow solid (280 mg, 63%). Compound **5** (280 mg, 1.26 mmol) was dissolved in the mixture of methanol and ethyl acetate (8 mL, volume ratio = 1 : 1), Pd/C (10% Pd, 28 mg) was then added. The mixture was stirred under hydrogen atmosphere for 6 h at room temperature. Pd/C was filtered by diatomite and the solvents were removed under reduced pressure to afford compound **6** as a gray solid (230 mg, 95%).

### Preparation of 2-chloro-5-fluoro-*N*-substituted-pyrimidin-4-amine and 2-chloro-*N*-substituted-5-nitropyrimidin-4-amine (8)

2,4-Dichloro-5-fluoropyrimidine (**7a**: $R^2$ = F, 334 mg, 2 mmol), *p*-anisidine (246 mg, 2 mmol) were mixed in 3 mL ethanol, and triethylamine (304 mg, 3 mmol) was then added. The mixture was stirred for 5 h at room temperature. The solvent was removed under reduced pressure and the crude material was washed by ethyl ether to give **8a** as a gray solid (374 mg, 74%). Compounds **8b–8d** and **8h** were synthesized from different starting materials with procedures similar to that of **8a**.

Compound **7a** (1.67 g, 10 mmol) and 2,6-difluoroaniline (1.29 g, 10 mmol) were dissolved in the mixture of methanol and $H_2O$ (4 : 1). The mixture was stirred at room temperature for 48 h, and the precipitation was filtered and dried to afford compound **8e** as a white solid (900 mg, 35%). **8f** and **8g** were synthesized from different starting materials with procedures similar to that of **8e**. Compound **8i** was synthesized from 2,4-dichloro-5-nitro-pyrimidine (**7b**: $R^2$ = $NO_2$) using procedure similar to that of **8e**.

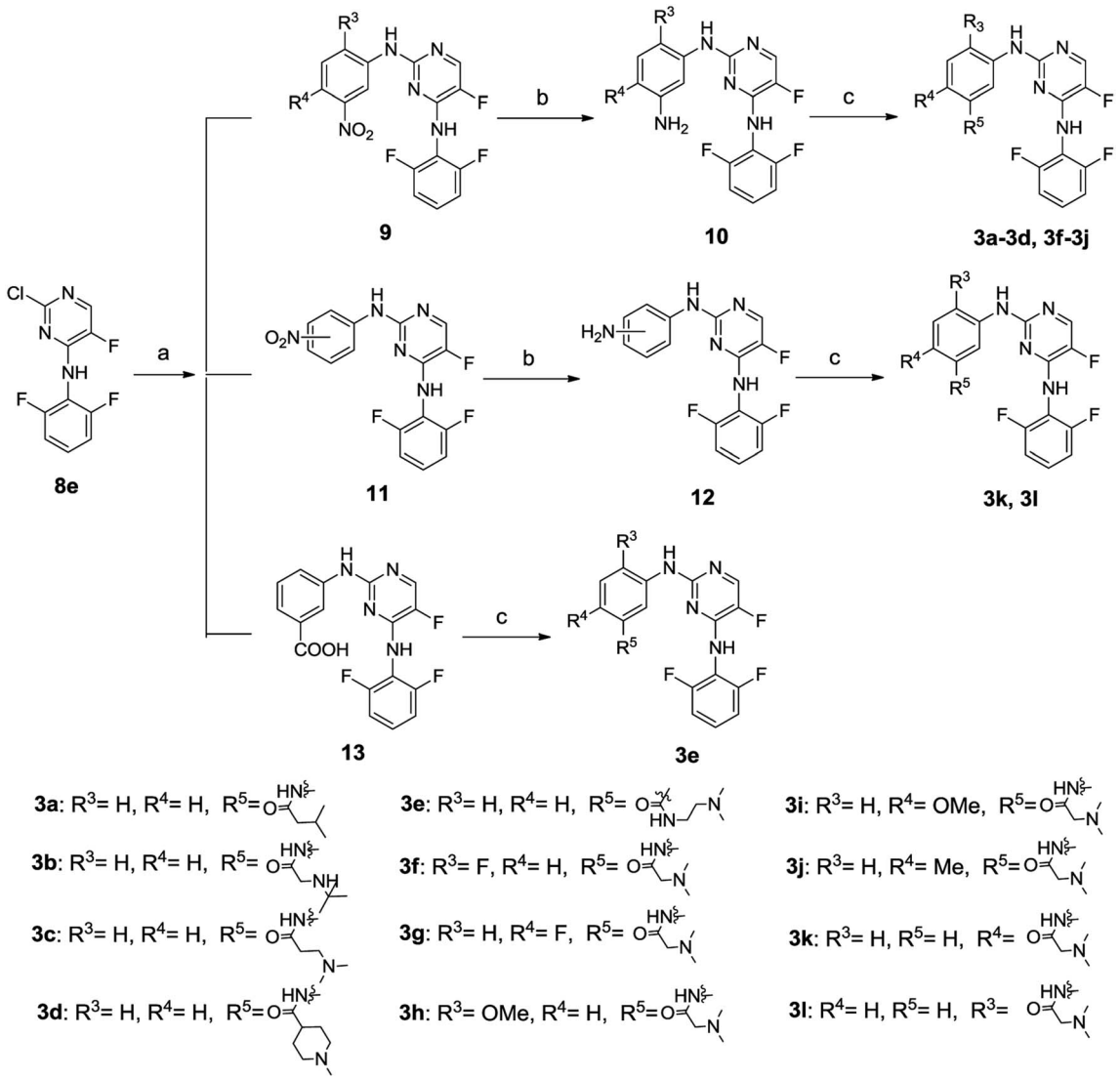


Scheme 2 Synthesis of compounds **3a–3l**. *Reagents and conditions: (a) appropriate amine, X-phos, $Pd_2(dba)_3$, $K_2CO_3$, dry toluene, *t*-butanol, $N_2$, microwave irradiation, 49–70%; (b) Pd/C, $H_2$, $CH_3OH$/ethyl acetate, 73–95%; (c) appropriate amine, HATU, DIEA, DMF, 22–74%.

**General procedure for the preparation of (2)**

Compound **6** (96 mg, 0.5 mmol), compound **8a** (126 mg, 0.5 mmol), xantphos (29 mg, 0.05 mmol), $Pd(OAc)_2$ (6 mg, 0.025 mmol) and $Cs_2CO_3$ (489 mg, 1.5 mmol) were added to anhydrous THF (2 mL). Nitrogen was bubbled through the reaction mixture for 5 min, and then the reaction vessel was sealed and heated under microwave irradiation to 130 °C for 25 min. The mixture was filtered and the filtrate was concentrated under vacuum. The crude product was purified by silica gel chromatography, and eluted with petroleum ether/ethyl acetate (6 : 1) to give **2a** as a white solid (104 mg, 50%).

Compounds **2b–2i** were synthesized from different starting materials using the same procedure as described for **2a**.

**2-(Dimethylamino)-*N*-(3-((5-fluoro-4-((4-methoxyphenyl) amino)pyrimidin-2-yl)amino)phenyl)acetamide (2a).** Yield: 50%, mp: 183–185 °C; $^1$H NMR (400 MHz, DMSO-d6) $\delta$ 9.64 (s, 1H), 9.20 (s, 1H), 9.13 (s, 1H), 8.04 (d, $J$ = 3.6 Hz, 1H), 7.81 (s, 1H), 7.70 (d, $J$ = 8.8 Hz, 2H), 7.41 (d, $J$ = 8.0 Hz, 1H), 7.19 (d, $J$ = 8.0 Hz, 1H), 7.12 (t, $J$ = 8.0 Hz, 1H), 6.89 (d, $J$ = 8.8 Hz, 2H), 3.75 (s, 3H), 3.19 (s, 2H), 2.35 (s, 6H); $^{13}$C NMR (100 MHz, $CDCl_3$) $\delta$ 168.9, 156.5, 155.5 (d, $J_{C-F}$ = 3 Hz), 150.4 (d, $J_{C-F}$ = 10 Hz), 142.5, 139.9 (d, $J_{C-F}$ = 20 Hz), 139.5 (d, $J_{C-F}$ = 240 Hz), 139.8, 130.8, 129.4, 123.1 (2C), 114.9, 114.2 (2C), 113.3, 110.1, 63.8, 55.6, 46.1 (2C); HR-ESI-MS: $m/z$ = 411.1929 $[M + H]^+$, calcd for $C_{21}H_{24}FN_6O_2$: 411.1939.

***N*-(3-((4-((4-Acetylphenyl)amino)-5-fluoropyrimidin-2-yl) amino)phenyl)-2-(dimethylamino)acetamide (2b).** Yield: 46%, mp: 215–216 °C, $^1$H NMR (300 MHz, $CDCl_3$) $\delta$ 9.23 (s, 1H), 8.05 (d, $J$ = 3.0 Hz, 1H), 7.95 (d, $J$ = 8.7 Hz, 2H), 7.92 (s, 1H), 7.76 (d, $J$ = 8.7 Hz, 2H), 7.41 (d, $J$ = 7.5 Hz, 1H), 7.30 (d, $J$ = 8.1 Hz, 1H), 7.20 (d, $J$ = 7.8 Hz, 1H), 7.05 (s, 2H), 3.14 (s, 2H), 2.59 (s, 3H), 2.41 (s, 6H); $^{13}$C NMR (100 MHz, $CDCl_3$) $\delta$ 196.8, 168.6, 155.4 (d, $J_{C-F}$ = 4 Hz), 149.3 (d, $J_{C-F}$ = 10 Hz), 142.4, 141.3 (d, $J_{C-F}$ = 226 Hz), 141.1 (d, $J_{C-F}$ = 20 Hz), 139.9, 138.3, 132.2, 129.7 (2C), 129.4, 119.2 (2C), 115.5,

 

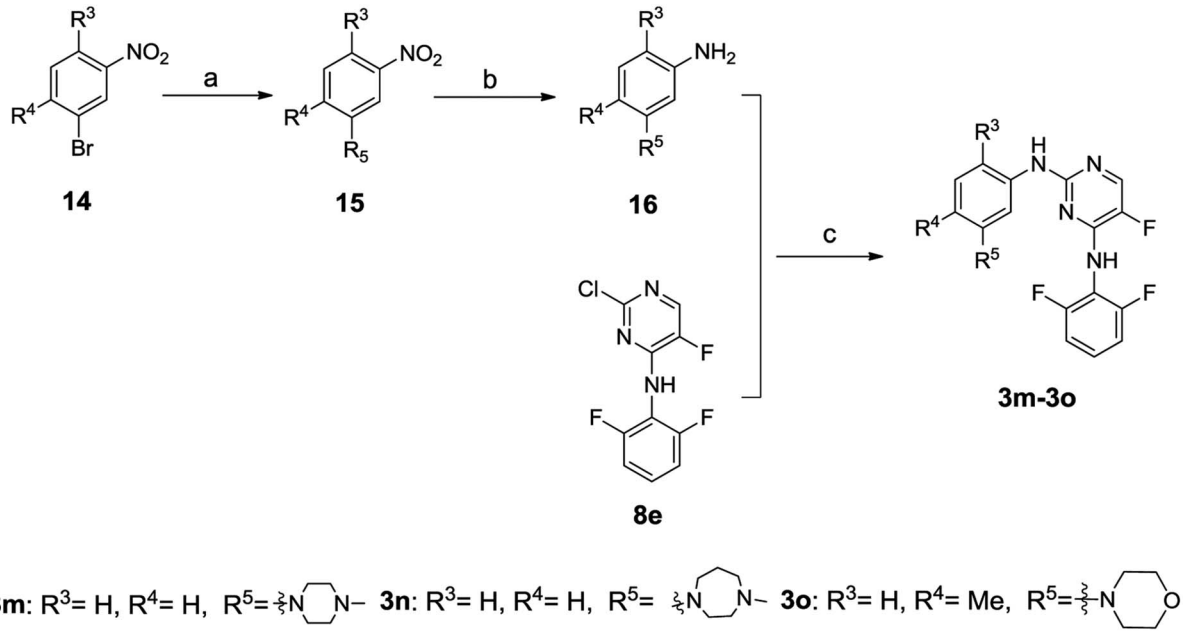


Scheme 3 Synthesis of compounds **3m–3o**. *Reagents and conditions: (a) appropriate amine, 2,2′-bis(diphenylphosphino)-1,1′-binaphthyl (BINAP), $Pd(OAc)_2$, $Cs_2CO_3$, dry toluene, $N_2$, reflux, 60–72%; (b) Pd/C, $H_2$, $CH_3OH$/ethyl acetate, 80–89%; (c) Tris(dibenzylideneacetone) dipalladium (0) ($Pd_2(dba)_3$), X-phos, $K_2CO_3$, toluene, *t*-butanol, $N_2$, microwave irradiation, 34–51%.

113.8, 110.7, 63.6, 45.9 (2C), 26.4; HR-ESI-MS: $m/z = 423.1930$ $[M + H]^+$, calcd for $C_{22}H_{24}FN_6O_2$: 423.1939.

***N*-(3-((4-((4-Chlorophenyl)amino)-5-fluoropyrimidin-2-yl) amino)phenyl)-2-(dimethylamino)acetamide (2c).** Yield: 20%, mp: 222–224 °C, $^1H$ NMR (400 MHz, $CDCl_3$) $\delta$ 9.14 (s, 1H), 7.99

Table 3 Inhibitory activities of selected compounds against tumor cell lines by the SRB assay

| | $GI_{50}$[a] (μM) | | | | |
|---|---|---|---|---|---|
| Compd. | MDA-MB-231 | MCF-7 | A549 | KB | KB-vin[b] |
| **1** | — | — | 1.18 ± 0.13 | 1.26 ± 0.05 | 1.81 ± 0.60 |
| **2a** | 1.20 ± 0.06 | 0.67 ± 0.06 | 0.72 ± 0.01 | 0.57 ± 0.01 | 2.54 ± 0.01 |
| **2b** | 5.80 ± 0.08 | 3.80 ± 0.24 | 2.33 ± 0.03 | 2.20 ± 0.37 | 5.99 ± 0.26 |
| **2c** | 6.77 ± 0.38 | 3.94 ± 0.31 | 2.12 ± 0.26 | 2.03 ± 0.32 | 3.90 ± 0.07 |
| **2d** | 1.64 ± 0.15 | 2.83 ± 0.03 | 1.89 ± 0.19 | 3.08 ± 0.16 | 3.20 ± 0.18 |
| **2e** | 3.98 ± 0.16 | 4.49 ± 0.03 | 1.31 ± 0.07 | 4.78 ± 0.38 | 2.54 ± 0.26 |
| **2f** | 12.99 ± 0.38 | 6.02 ± 0.51 | 3.47 ± 0.44 | 7.04 ± 0.08 | 4.54 ± 0.04 |
| **2g** | 4.64 ± 0.06 | 0.67 ± 0.03 | 0.71 ± 0.06 | 0.56 ± 0.08 | 1.66 ± 0.16 |
| **2h** | >10[c] | >10 | >10 | >10 | >10 |
| **2i** | 5.94 ± 0.33 | 10.23 ± 0.03 | 4.90 ± 0.45 | 5.73 ± 0.35 | 5.98 ± 0.24 |
| **3a** | >10 | 5.97 ± 0.19 | 0.72 ± 0.04 | 0.59 ± 0.05 | 1.66 ± 0.16 |
| **3b** | 2.07 ± 0.12 | 2.73 ± 0.48 | 1.31 ± 0.18 | 3.27 ± 0.13 | 2.36 ± 0.33 |
| **3c** | 3.24 ± 0.05 | 2.65 ± 0.40 | 1.20 ± 0.05 | 2.31 ± 0.11 | 6.34 ± 0.54 |
| **3d** | 3.30 ± 0.23 | 6.16 ± 0.14 | 1.09 ± 0.03 | 2.60 ± 0.45 | 7.11 ± 0.23 |
| **3e** | 5.42 ± 0.35 | 6.73 ± 0.23 | 0.72 ± 0.01 | 3.82 ± 0.11 | 11.64 ± 0.04 |
| **3g** | 5.51 ± 0.16 | 3.98 ± 0.26 | 0.69 ± 0.002 | 3.89 ± 0.06 | 0.98 ± 0.13 |
| **3i** | 4.05 ± 0.14 | 1.88 ± 0.12 | 0.70 ± 0.002 | 2.87 ± 0.24 | 1.09 ± 0.06 |
| **3j** | 5.31 ± 0.19 | 2.37 ± 0.62 | 1.15 ± 0.08 | 0.60 ± 0.04 | 0.88 ± 0.01 |
| **3k** | 6.01 ± 0.08 | 4.48 ± 0.39 | 3.04 ± 0.18 | 3.80 ± 0.34 | 4.52 ± 0.01 |
| **3m** | 2.84 ± 0.67 | 7.76 ± 0.52 | 1.25 ± 0.08 | 0.40 ± 0.09 | 3.70 ± 0.53 |
| **3n** | 4.77 ± 0.27 | 7.16 ± 0.54 | 0.71 ± 0.01 | 4.44 ± 0.42 | 0.95 ± 0.001 |
| **3o** | 7.00 ± 0.06 | 3.75 ± 0.28 | 0.85 ± 0.01 | 0.98 ± 0.05 | 0.84 ± 0.02 |
| FVP[d] | — | — | 0.14 ± 0.01 | 0.16 ± 0.01 | 0.18 ± 0.01 |
| Paclitaxel (nM) | 7.76 ± 0.39 | 8.78 ± 0.79 | 5.98 ± 0.40 | 4.94 ± 0.21 | 1518.36 ± 141.54 |

[a] The $GI_{50}$ values are expressed as means ± SD (standard deviation) of three independent measurements. [b] Cell lines: MDA-MB-231 (human breast carcinoma cell line), MCF-7 (Michigan Cancer Foundation-7), A549 (lung cancer), KB (nasopharyngeal carcinoma) and KB-vin (vincristine-resistant KB subline). [c] No significant inhibition against tumor cell growth was observed under the concentration of 10 μM. [d] The data were cited from ref. 16.

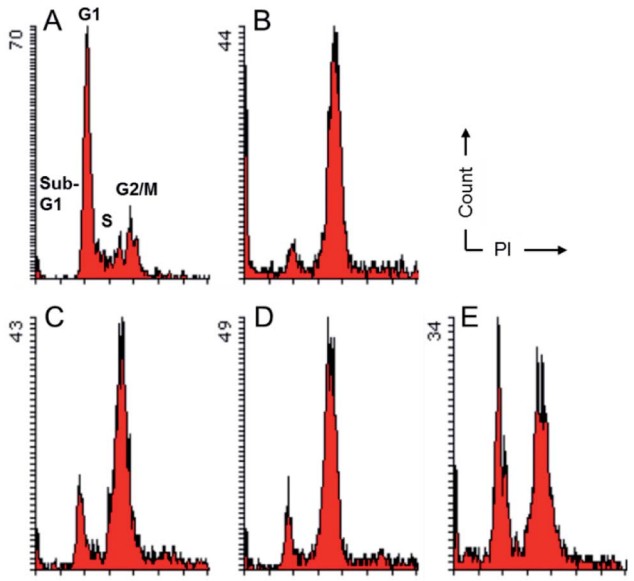


Fig. 3 Effects of compounds **2a**, **2d** and **3b** on cell cycle progression. MDA-MB-231 cells were treated for 24 h with compounds at a concentration five-fold $GI_{50}$. Cells were fixed and stained with propidium iodide (PI) followed by cell cycle analysis using a flow cytometer. DMSO (A) and 200 nM combretastatin A-4 (CA-4) (B) were used as negative and positive control, respectively, for induction of cell cycle arrest in G2/M. Compounds **2a** at 6.0 μM (C), **2d** at 8.0 μM (D) or **3b** at 10.5 μM (E) were used.

(d, $J$ = 3.2 Hz, 1H), 7.86 (s, 1H), 7.59 (d, $J$ = 8.8 Hz, 2H), 7.33–7.35 (m, 1H), 7.29 (d, $J$ = 8.8 Hz, 2H), 7.24 (s, 1H), 7.21–7.23 (m, 1H), 7.00 (s, 1H), 6.80 (s, 1H), 3.12 (s, 2H), 2.40 (s, 6H); $^{13}$C NMR (100 MHz, DMSO-d6) $\delta$ 168.9, 156.0 (d, $J_{C-F}$ = 2 Hz), 149.8 (d, $J_{C-F}$ = 10 Hz), 142.4, 141.2 (d, $J_{C-F}$ = 20 Hz), 140.3 (d, $J_{C-F}$ = 236 Hz), 139.9, 138.7, 128.9, 128.8 (2C), 126.9, 122.8 (2C), 115.2, 113.6, 111.4, 63.7, 45.9 (2C); HR-ESI-MS: $m/z$ = 415.1435 [M + H]$^+$, calcd for $C_{20}H_{21}ClFN_6O$: 415.1444.

**2-(Dimethylamino)-*N*-(3-((4-((4-(dimethylamino)phenyl)amino)-5-fluoropyrimidin-2-yl)amino)phenyl)acetamide (2d).** Yield: 24%, mp: 162–163 °C, $^1$H NMR (400 MHz, $CDCl_3$) $\delta$ 9.09 (s, 1H), 7.91 (d, $J$ = 3.2 Hz, 1H), 7.76 (s, 1H), 7.43 (d, $J$ = 8.8 Hz, 3H), 7.22 (s, 1H), 7.21 (s, 1H), 6.96 (s, 1H), 6.74 (d, $J$ = 8.8 Hz, 2H), 6.62 (s, 1H), 3.10 (s, 2H), 3.03 (s, 6H), 2.38 (s, 6H); $^{13}$C NMR (100 MHz, $CDCl_3$) $\delta$ 168.6, 155.4 (d, $J_{C-F}$ = 3 Hz), 150.6 (d, $J_{C-F}$ = 10 Hz), 148.1, 142.5, 140.1, 139.4 (d, $J$C–F = 255 Hz), 139.3 (d, $J_{C-F}$ = 20 Hz), 129.3, 127.1, 123.2 (2C), 114.7, 113.0, 112.9 (2C), 109.8, 63.7, 45.9 (2C), 40.9 (2C); HR-ESI-MS: $m/z$ = 424.2244 [M + H]$^+$, calcd for $C_{22}H_{27}FN_7O$: 424.2256.

***N*-(3-((4-((2,6-Difluorophenyl)amino)-5-fluoropyrimidin-2-yl)-amino)phenyl)-2-(dimethylamino)acetamide (2e).** Yield: 53%, mp: 172–174 °C, $^1$H NMR (400 MHz, $CDCl_3$) $\delta$ 9.09 (s, 1H), 8.01 (d, $J$ = 2.8 Hz, 1H), 7.65 (s, 1H), 7.30 (d, $J$ = 8.8 Hz, 1H), 7.23–7.25 (m, 1H), 7.18 (d, $J$ = 8.0 Hz, 1H), 7.11 (t, $J$ = 8.0 Hz, 1H), 7.03 (t, $J$ = 8.0 Hz, 2H), 6.90 (s, 1H), 6.33 (s, 1H), 3.13 (s, 2H), 2.42 (s, 6H); $^{13}$C NMR (100 MHz, $CDCl_3$) $\delta$ 168.8, 158.4 (dd, $J_{C-F}$ = 249 Hz, 4 Hz, 2C), 155.6 (d, $J_{C-F}$ = 3 Hz), 150.7 (d, $J_{C-F}$ = 11 Hz), 141.6 (d, $J_{C-F}$ = 246 Hz), 141.2 (d, $J_{C-F}$ = 19 Hz), 140.6, 138.1, 129.2, 127.5 (t, $J_{C-F}$ = 10 Hz), 114.5 (t, $J_{C-F}$ = 16 Hz), 114.5, 113.1, 111.8 (dd, $J_{C-F}$ = 19 Hz, 6 Hz, 2C), 109.6, 63.8, 46.1 (2C); HR-ESI-MS: $m/z$ = 417.1633 [M + H]$^+$, calcd for $C_{20}H_{20}F_3N_6O$: 417.1645.

***N*-(3-((4-((2,6-Dichlorophenyl)amino)-5-fluoropyrimidin-2-yl)-amino)phenyl)-2-(dimethylamino)acetamide (2f).** Yield: 57%, mp: 179–181 °C, $^1$H NMR (400 MHz, DMSO-d6) $\delta$ 9.44 (s, 1H), 9.34 (s, 1H), 9.07 (s, 1H), 8.09 (d, $J$ = 3.6 Hz, 1H), 7.61 (s, 1H), 7.59 (s, 1H), 7.49 (s, 1H), 7.41 (t, $J$ = 8.0 Hz, 1H), 7.12–7.17 (m, 2H), 6.87 (t, $J$ = 8.0 Hz, 1H), 3.04 (s, 2H), 2.27 (s, 6H); $^{13}$C NMR (100 MHz, $CDCl_3$) $\delta$ 168.7, 155.3 (d, $J_{C-F}$ = 3 Hz), 150.5 (d, $J_{C-F}$ = 11 Hz), 141.4 (d, $J_{C-F}$ = 245 Hz), 141.1 (d, $J_{C-F}$ = 19 Hz), 140.4, 138.0, 134.3 (2C), 132.5, 129.2, 128.5 (2C), 128.4, 114.2, 113.0, 109.3, 63.7, 46.0 (2C); HR-ESI-MS: $m/z$ = 449.1045 [M + H]$^+$, calcd for $C_{20}H_{20}FCl_2N_6O$: 449.1054.

***N*-(3-((4-((3,5-Difluorophenyl)amino)-5-fluoropyrimidin-2-yl)-amino)phenyl)-2-(dimethylamino)acetamide (2g).** Yield: 38%, mp: 190–192 °C, $^1$H NMR (400 MHz, DMSO-d6) $\delta$ 9.66 (s, 1H), 9.57 (s, 1H), 9.41 (s, 1H), 8.19 (d, $J$ = 3.6 Hz, 1H), 7.89 (s, 1H), 7.71 (d, $J$ = 8.8 Hz, 2H), 7.40 (d, $J$ = 8.4 Hz, 1H), 7.23 (d, $J$ = 8.4 Hz, 1H), 7.17 (t, $J$ = 8.0 Hz, 1H), 6.83 (t, $J$ = 9.2 Hz, 1H), 3.06

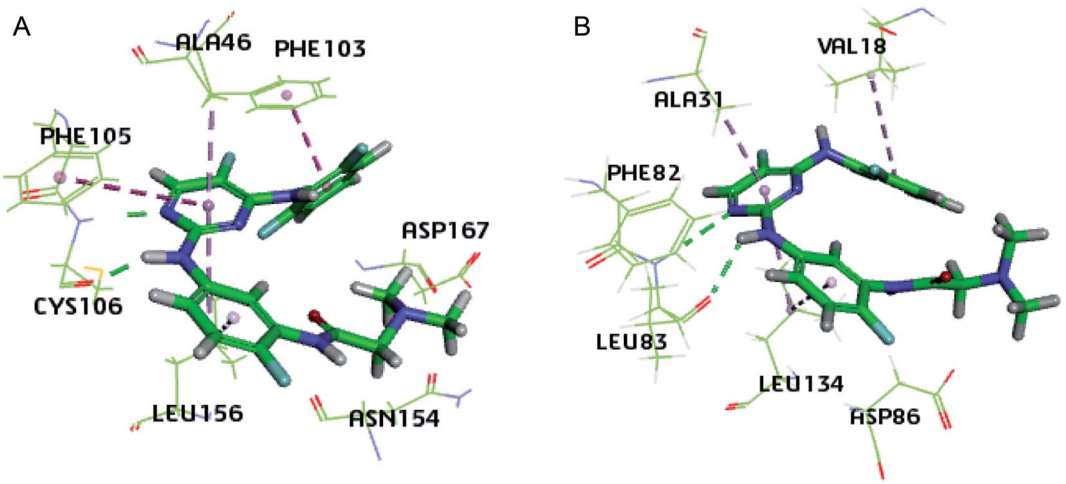


Fig. 4 Interaction modes of **3g** with CDK9 (A) and CDK2 (B) as suggested by the docking study. Green dashed lines indicate hydrogen bonds, deep purple dashed lines represent π–π stacking interactions and hydrophobic interactions are shown as light purple dashed lines.

(s, 2H), 2.27 (s, 6H); $^{13}$C NMR (100 MHz, $CDCl_3$) $\delta$ 168.8, 163.3 (dd, $J_{C-F}$ = 245 Hz, 14 Hz, 2C), 155.4 (d, $J_{C-F}$ = 3 Hz), 149.4 (d, $J_{C-F}$ = 10 Hz), 141.1 (d, $J_{C-F}$ = 19 Hz), 140.9 (d, $J_{C-F}$ = 247 Hz), 140.2 (t, $J_{C-F}$ = 14 Hz), 140.0, 138.4, 129.5, 115.5, 113.9, 110.7, 103.0 (dd, $J_{C-F}$ = 21 Hz, 9 Hz, 2C), 98.7 (t, $J_{C-F}$ = 26 Hz), 63.7, 46.0 (2C); HR-ESI-MS: $m/z$ = 417.1636 $[M + H]^+$, calcd for $C_{20}H_{20}F_3N_6O$: 417.1645.

**2-(Dimethylamino)-*N*-(3-((5-fluoro-4-((4-methylpiperazin-1-yl)-amino)pyrimidin-2-yl)amino)phenyl)acetamide (2h).** Yield: 42%, mp: 165–167 °C, $^1$H NMR (400 MHz, $CDCl_3$) $\delta$ 9.06 (s, 1H), 7.82–7.95 (m, 2H), 7.45 (d, $J$ = 8.0 Hz, 1H), 7.24 (d, $J$ = 8.0 Hz, 1H), 7.21 (s, 1H), 7.18 (d, $J$ = 8.0 Hz, 1H), 5.76 (s, 1H), 3.06 (s, 2H), 2.98 (s, 4H), 2.66 (s, 4H), 2.37 (s, 6H), 2.36 (s, 3H); $^{13}$C NMR (100 MHz, $CDCl_3$) $\delta$ 168.8, 155.9, 151.6 (d, $J_{C-F}$ = 9 Hz), 140.5 (d, $J_{C-F}$ = 245 Hz), 141.0, 139.9 (d, $J_{C-F}$ = 19 Hz), 138.3, 129.4, 114.4, 113.0, 109.6, 63.9, 55.5 (2C), 54.4 (2C), 46.1 (2C), 45.8; HR-ESI-MS: $m/z$ = 403.2354 $[M + H]^+$, calcd for $C_{19}H_{28}FN_8O$: 403.2365.

***N*-(3-((4-((2,6-Difluorophenyl)amino)-5-nitropyrimidin-2-yl)-amino)phenyl)-2-(dimethylamino)acetamide (2i).** Yield: 20%, mp: 218–220 °C, $^1$H NMR (400 MHz, DMSO-d6) $\delta$ 10.47 (s, 1H), 10.06 (s, 1H), 9.51 (s, 1H), 9.09 (s, 1H), 7.44–7.54 (m, 2H), 7.26 (t, $J$ = 8.0 Hz, 2H), 7.22 (s, 1H), 7.15 (d, $J$ = 7.2 Hz, 1H), 6.84 (s, 1H), 3.07 (s, 2H), 2.28 (s, 6H); $^{13}$C NMR (100 MHz, DMSO-d6) $\delta$ 169.4, 159.8, 158.7 (dd, $J_{C-F}$ = 248 Hz, 4 Hz, 2C), 158.1, 155.8, 139.0, 138.6, 138.1, 129.7 (t, $J_{C-F}$ = 10 Hz), 129.1, 129.0, 121.6, 115.9, 114.9 (t, $J_{C-F}$ = 16 Hz), 112.4 (dd, $J_{C-F}$ = 18 Hz, 4 Hz, 2C), 63.1, 45.5 (2C); HR-ESI-MS: $m/z$ = 444.1580 $[M + H]^+$, calcd for $C_{20}H_{20}F_2N_7O_3$: 444.1590.

### Preparation of $N^4$-(2,6-difluorophenyl)-5-fluoro-$N^2$-(substituted-phenyl)pyrimidine-2,4-diamine (9) (11) (13)

Compound **8e** (518 mg, 2 mmol), 3-nitroaniline (276 mg, 2 mmol), X-phos (95 mg, 0.2 mmol), $Pd_2(dba)_3$ (92 mg, 0.1 mmol), and $Cs_2CO_3$ (1.95 g, 6 mmol) were added to toluene (2 mL) and tertiary butanol (2 mL). Nitrogen was bubbled through the reaction mixture for 5 min, and then the reaction vessel was sealed and heated under microwave irradiation to 120 °C for 25 min. The mixture was filtered and the filtrate was concentrated under vacuum. The crude product was washed by petroleum ether and DCM (4 : 1) to provide **9a** as a yellow solid (350 mg, 49%) for the next step.

Compounds **9b–9d**, **9f–9j**, **11**, **13** were prepared from **8e** and other different starting materials with the same procedure as described for **9a**.

### Preparation of $N^4$-(2,6-difluorophenyl)-5-fluoro-$N^2$-(substituted-phenyl)pyrimidine-2,4-diamine (10) (12)

Compound **9a** (150 mg, 0.42 mmol) was dissolved in the mixture of methanol and ethyl acetate (6 mL, 1 : 1), Pd/C (10% Pd, 15 mg) was then added. The mixture was stirred under hydrogen atmosphere for 6 h at room temperature. Pd/C was filtered by diatomite and the solvents were removed under reduced pressure to afford compound **10a** as a gray solid (100 mg, 73%). Compounds **10b–10d**, **10f–10j** and **12** were prepared from different starting materials with the same procedure as described for **10a**.

### General procedure for the preparation of (3a–3l)

Compound **10a** (100 mg, 0.3 mmol) and isopentanoic acid (34 mg, 0.33 mmol) were dissolved in 3 mL DMF. HATU (137 mg, 0.36 mmol) and DIEA (194 mg, 1.5 mmol) were then added. The reaction mixture was stirred at room temperature overnight. After the solvent was evaporated, the residue was dissolved in ethyl acetate and then washed with saturated sodium bicarbonate. The organic layer was concentrated and the crude material was purified by column chromatography on silica gel to afford compound **3a** as a white solid (65 mg, 52%).

Compounds **3b–3l** were prepared from respective starting materials with the same procedure as described for **3a**.

***N*-(3-((4-((2,6-Difluorophenyl)amino)-5-fluoropyrimidin-2-yl)-amino)phenyl)-3-methylbutanamide (3a).** Yield: 52%, mp: 178–180 °C, $^1$H NMR (400 MHz, DMSO-d6) $\delta$ 9.63 (s, 1H), 9.21 (s, 1H), 9.09 (s, 1H), 8.10 (d, $J$ = 3.2 Hz, 1H), 7.52 (s, 1H), 7.38–7.45 (m, 1H), 7.20–7.25 (m, 3H), 7.11 (d, $J$ = 8.0 Hz, 1H), 6.89 (t, $J$ = 8.0 Hz, 1H), 2.15 (d, $J$ = 6.8 Hz, 2H), 2.00–2.08 (m, 1H), 0.91 (d, $J$ = 6.4 Hz, 6H); $^{13}$C NMR (100 MHz, CD3OD) $\delta$ 170.4, 157.0 (dd, $J_{C-F}$ = 248 Hz, 5 Hz, 2C), 153.70 (d, $J_{C-F}$ = 1 Hz), 149.4 (d, $J_{C-F}$ = 12 Hz), 139.1 (d, $J_{C-F}$ = 243 Hz), 138.7, 137.8 (d, $J_{C-F}$ = 19 Hz), 136.2, 126.0, 125.4 (t, $J_{C-F}$ = 10 Hz), 112.9 (t, $J_{C-F}$ = 17 Hz), 112.5, 111.5, 109.2 (dd, $J_{C-F}$ = 18 Hz, 5 Hz, 2C), 108.8, 43.6, 24.0, 19.2 (2C); HR-ESI-MS: $m/z$ = 416.1684 $[M + H]^+$, calcd for $C_{21}H_{21}F_3N_5O$: 416.1693.

**2-(*tert*-Butylamino)-*N*-(3-((4-((2,6-difluorophenyl)amino)-5-fluoropyrimidin-2-yl)amino)phenyl)acetamide (3b).** Yield: 53%, mp: 172–174 °C, 1H NMR (400 MHz, DMSO-d6) $\delta$ 9.60 (s, 1H), 9.23 (s, 1H), 9.12 (s, 1H), 8.11 (d, $J$ = 3.2 Hz, 1H), 7.48 (s, 1H), 7.38–7.44 (m, 1H), 7.26 (s, 1H), 7.22 (d, $J$ = 8.4 Hz, 2H), 7.17 (d, $J$ = 8.4 Hz, 1H), 6.94 (t, $J$ = 8.4 Hz, 1H), 3.20 (s, 2H), 1.05 (s, 9H); $^{13}$C NMR (100 MHz, DMSO-d6) $\delta$ 167.0, 159.3 (dd, $J_{C-F}$ = 246 Hz, 5 Hz, 2C), 156.2 (d, $J_{C-F}$ = 2 Hz), 151.4 (d, $J_{C-F}$ = 12 Hz), 141.9, 141.5 (d, $J_{C-F}$ = 19 Hz), 141.4 (d, $J_{C-F}$ = 245 Hz), 138.5, 129.0, 128.7 (t, $J_{C-F}$ = 10 Hz), 115.5 (t, $J_{C-F}$ = 17 Hz), 114.5, 112.7, 112.6 (dd, $J_{C-F}$ = 18 Hz, 5 Hz, 2C), 110.0, 54.5, 44.8, 26.9 (3C); HR-ESI-MS: $m/z$ = 445.1946 $[M + H]^+$, calcd for $C_{22}H_{24}F_3N_6O$: 445.1958.

***N*-(3-((4-((2,6-Difluorophenyl)amino)-5-fluoropyrimidin-2-yl)-amino)phenyl)-3-(dimethylamino)propanamide (3c).** Yield: 61%, mp: 190–192 °C, $^1$H NMR (400 MHz, DMSO-d6) $\delta$ 9.89 (s, 1H), 9.22 (s, 1H), 9.13 (s, 1H), 8.10 (d, $J$ = 3.6 Hz, 1H), 7.52 (s, 1H), 7.38–7.46 (m, 1H), 7.20–7.26 (m, 3H), 7.13 (d, $J$ = 7.6 Hz, 1H), 6.92 (t, $J$ = 8.0 Hz, 1H), 2.84 (s, 2H), 2.55 (t, $J$ = 6.8 Hz, 2H), 2.41 (s, 6H); $^{13}$C NMR (100 MHz, CD3OD) $\delta$ 171.9, 160.7 (dd, $J_{C-F}$ = 248 Hz, 5 Hz, 2C), 157.3 (d, $J_{C-F}$ = 2 Hz), 153.0 (d, $J_{C-F}$ = 11 Hz), 142.7 (d, $J_{C-F}$ = 245 Hz), 142.4, 141.3 (d, $J_{C-F}$ = 20 Hz), 139.7, 129.7, 129.0 (t, $J_{C-F}$ = 10 Hz), 116.5 (t, $J_{C-F}$ = 11 Hz), 116.1, 114.8, 112.8 (dd, $J_{C-F}$ = 19 Hz, 6 Hz, 2C), 112.1, 56.0, 44.9 (2C), 34.4; HR-ESI-MS: $m/z$ = 431.1792 $[M + H]^+$, calcd for $C_{21}H_{22}F_3N_6O$: 431.1802.

***N*-(3-((4-((2,6-Difluorophenyl)amino)-5-fluoropyrimidin-2-yl) amino)phenyl)-1-methylpiperidine-4-carboxamide (3d).** Yield: 22%, mp: 184–186 °C, $^1$H NMR (400 MHz, DMSO-d6) $\delta$ 9.90 (s, 1H), 9.23 (s, 1H), 9.12 (s, 1H), 8.10 (s, 1H), 7.57 (s, 1H), 7.40–7.44 (m, 1H), 7.25 (s, 1H), 7.23 (d, $J$ = 8.0 Hz, 2H), 7.14 (d, $J$ = 8.0 Hz, 1H), 6.92 (t, $J$ = 8.4 Hz, 1H), 3.39 (s, 2H), 2.92 (s, 2H), 2.72 (s,

3H), 2.57 (s, 1H), 1.87–1.99 (m, 4H); 13C NMR (100 MHz, $CD_3OD$) $\delta$ 173.7, 160.6 (dd, $J_{C-F}$ = 248 Hz, 4 Hz, 2C), 157.2 (d, $J_{C-F}$ = 2 Hz), 153.1 (d, $J_{C-F}$ = 12 Hz), 143.7 (d, $J_{C-F}$ = 245 Hz), 142.3, 141.1 (d, $J_{C-F}$ = 20 Hz), 139.6, 129.7, 129.1 (t, $J_{C-F}$ = 10 Hz), 116.4 (t, $J_{C-F}$ = 17 Hz), 116.3, 114.9, 112.8 (dd, $J_{C-F}$ = 18 Hz, 5 Hz, 2C), 112.2, 54.9 (2C), 44.0, 41.5, 27.7 (2C); HR-ESI-MS: $m/z$ = 457.1950 $[M + H]^+$, calcd for $C_{23}H_{24}F_3N_6O$: 457.1958.

**3-((4-((2,6-Difluorophenyl)amino)-5-fluoropyrimidin-2-yl)-amino)-*N*-(2-(dimethylamino)ethyl)benzamide (3e).** Yield: 47%, mp: 190–192 °C, $^1$H NMR (400 MHz, $CDCl_3$) $\delta$ 8.01 (d, $J$ = 2.8 Hz, 1H), 7.53–7.81 (m, 2H), 7.34 (d, $J$ = 7.6 Hz, 1H), 7.28–7.30 (m, 1H), 7.21 (t, $J$ = 7.6 Hz, 1H), 7.03 (t, $J$ = 8.0 Hz, 2H), 6.93 (s, 1H), 6.82 (s, 1H), 6.33 (s, 1H), 3.54 (t, $J$ = 5.6 Hz, 2H), 2.55 (t, $J$ = 5.6 Hz, 2H), 2.30 (s, 6H); $^{13}$C NMR (125 MHz, $CDCl_3$) $\delta$ 167.6, 158.5 (dd, $J_{C-F}$ = 250 Hz, 5 Hz, 2C), 155.6 (d, $J_{C-F}$ = 3 Hz), 150.8 (d, $J_{C-F}$ = 11 Hz), 141.9 (d, $J_{C-F}$ = 246 Hz), 141.3 (d, $J_{C-F}$ = 19 Hz), 140.3, 135.6, 129.0, 127.7 (t, $J_{C-F}$ = 10 Hz), 121.5, 120.5, 117.6, 114.5 (t, $J_{C-F}$ = 15 Hz), 111.9 (dd, $J_{C-F}$ = 19 Hz, 4 Hz, 2C), 58.0, 45.3 (2C), 37.4; HR-ESI-MS: $m/z$ = 431.1797 $[M + H]^+$, calcd for $C_{21}H_{22}F_3N_6O$: 431.1802.

***N*-(3-((4-((2,6-Difluorophenyl)amino)-5-fluoropyrimidin-2-yl)-amino)-4-fluorophenyl)-2-(dimethylamino)acetamide (3f).** Yield: 55%, mp: 204–205 °C, $^1$H NMR (400 MHz, DMSO- d6) $\delta$ 9.50 (s, 1H), 9.16 (s, 1H), 8.46 (s, 1H), 8.03 (d, $J$ = 3.2 Hz, 1H), 7.68 (dd, $J$ = 7.2 Hz, 2.0 Hz, 1H), 7.30–7.38 (m, 2H), 7.14 (t, $J$ = 8.0 Hz, 2H), 7.00 (t, $J$ = 9.6 Hz, 1H), 3.04 (s, 2H), 2.27 (s, 6H); 13C NMR (100 MHz, $CDCl_3$) $\delta$ 168.7, 158.4 (dd, $J_{C-F}$ = 249 Hz, 4 Hz, 2C), 155.1 (d, $J_{C-F}$ = 3 Hz), 150.8 (d, $J_{C-F}$ = 12 Hz), 149.0 (d, $J_{C-F}$ = 249 Hz), 142.0 (d, $J_{C-F}$ = 247 Hz), 140.9 (d, $J_{C-F}$ = 19 Hz), 133.8 (d, $J_{C-F}$ = 2 Hz), 128.5 (d, $J_{C-F}$ = 11 Hz), 127.5 (t, $J_{C-F}$ = 10 Hz), 114.7 (d, $J_{C-F}$ = 20 Hz), 114.3 (t, $J_{C-F}$ = 16 Hz), 113.4 (d, $J_{C-F}$ = 7 Hz), 111.8 (dd, $J_{C-F}$ = 18 Hz, 5 Hz, 2C), 111.1, 63.8, 46.1 (2C); HR-ESI-MS: $m/z$ = 435.1542 [M + H]+, calcd for $C_{20}H_{19}F_4N_6O$: 435.1551.

***N*-(5-((4-((2,6-Difluorophenyl)amino)-5-fluoropyrimidin-2-yl)-amino)-2-fluorophenyl)-2-(dimethylamino)acetamide (3g).** Yield: 40%, mp: 169–171 °C, $^1$H NMR (400 MHz, $CDCl_3$) $\delta$ 9.41 (s, 1H), 8.14 (dd, $J$ = 6.8 Hz, 2.4 Hz, 1H), 7.99 (d, $J$ = 3.2 Hz, 1H), 7.42–7.46 (m, 1H), 7.23–7.32 (m, 1H), 7.02 (t, $J$ = 8.0 Hz, 2H), 6.85–6.90 (m, 2H), 6.27 (s, 1H), 3.15 (s, 2H), 2.42 (s, 6H); 13C NMR (100 MHz, $CDCl_3$) $\delta$ 168.9, 158.3 (dd, $J_{C-F}$ = 249 Hz, 5 Hz, 2C), 155.5 (d, $J_{C-F}$ = 3 Hz), 150.5 (d, $J_{C-F}$ = 12 Hz), 147.9 (d, $J_{C-F}$ = 238 Hz), 141.6 (d, $J_{C-F}$ = 246 Hz), 141.1 (d, $J_{C-F}$ = 19 Hz), 136.1 (d, $J_{C-F}$ = 3 Hz), 127.4 (t, $J_{C-F}$ = 10 Hz), 125.9 (d, $J_{C-F}$ = 11 Hz), 114.5 (d, $J_{C-F}$ = 19 Hz), 114.4 (t, $J_{C-F}$ = 16 Hz), 114.3 (d, $J_{C-F}$ = 7 Hz), 111.8 (d, $J_{C-F}$ = 6 Hz), 111.7 (dd, $J_{C-F}$ = 18 Hz, 5 Hz, 2C), 63.7, 46.0 (2C); HR-ESI-MS: $m/z$ = 435.1538 $[M + H]^+$, calcd for $C_{20}H_{19}F_4N_6O$: 435.1551.

***N*-(3-((4-((2,6-difluorophenyl)amino)-5-fluoropyrimidin-2-yl)-amino)-4-methoxyphenyl)-2-(dimethylamino)acetamide (3h).** Yield: 68%, mp: 200–202 °C, $^1$H NMR (400 MHz, $CDCl_3$) $\delta$ 8.73 (s, 1H), 8.10 (s, 1H), 8.04 (s, 1H), 7.52 (d, $J$ = 8.8 Hz, 1H), 7.43 (s, 1H), 7.21–7.24 (m, 1H), 7.06 (t, $J$ = 8.4 Hz, 2H), 6.79 (d, $J$ = 8.8 Hz, 1H), 6.34 (s, 1H), 3.83 (s, 3H), 3.12 (s, 2H), 2.42 (s, 6H); 13C NMR (100 MHz, $CDCl_3$) $\delta$ 168.4, 158.2 (dd, $J_{C-F}$ = 249 Hz, 4 Hz, 2C), 155.4 (d, $J_{C-F}$ = 3 Hz), 150.5 (d, $J_{C-F}$ = 11 Hz), 144.5, 141.6 (d, $J_{C-F}$ = 246 Hz), 141.0 (d, $J_{C-F}$ = 19 Hz), 130.8, 129.6, 127.2 (t, $J_{C-F}$ = 10 Hz), 114.5 (t, $J_{C-F}$ = 16 Hz), 113.1, 111.7 (dd, $J_{C-F}$ = 18 Hz, 5 Hz, 2C), 110.0, 109.6, 63.8, 55.9, 46.1 (2C); HR-ESI-MS: $m/z$ = 447.1739 $[M + H]^+$, calcd for $C_{21}H_{22}F_3N_6O_2$: 447.1751.

***N*-(5-((4-((2,6-Difluorophenyl)amino)-5-fluoropyrimidin-2-yl)-amino)-2-methoxyphenyl)-2-(dimethylamino)acetamide (3i).** Yield: 36%, mp: 203–205 °C, 1H NMR (400 MHz, $CDCl_3$) $\delta$ 9.48 (s, 1H), 8.21 (d, $J$ = 2.8 Hz, 1H), 7.97 (d, $J$ = 2.8 Hz, 1H), 7.44 (dd, $J$ = 8.8 Hz, 2.4 Hz, 1H), 7.22–7.29 (m, 1H), 7.01 (t, $J$ = 7.6 Hz, 2H), 6.74 (s, 1H), 6.71 (d, $J$ = 8.8 Hz, 1H), 6.24 (s, 1H), 3.84 (s, 3H), 3.11 (s, 2H), 2.40 (s, 6H); $^{13}$C NMR (125 MHz, $CDCl_3$) $\delta$ 167.6, 158.5 (dd, $J_{C-F}$ = 250 Hz, 5 Hz, 2C), 155.6 (d, $J_{C-F}$ = 3 Hz), 150.8 (d $J_{C-F}$ = 11 Hz), 141.9 (d, $J_{C-F}$ = 246 Hz), 141.3 (d, $J_{C-F}$ = 19 Hz), 140.3, 135.6, 129.0, 127.7 (t, $J_{C-F}$ = 10 Hz), 121.5, 120.5, 117.6, 114.5 (t, $J_{C-F}$ = 15 Hz), 111.9 (dd, $J$ = 19 Hz, 4 Hz, 2C), 58.0, 45.3 (2C), 37.4; HR-ESI MS: $m/z$ = 447.1734 $[M + H]^+$, calcd for $C_{21}H_{22}F_3N_6O_2$: 447.1751.

***N*-(5-((4-((2,6-Difluorophenyl)amino)-5-fluoropyrimidin-2-yl)-amino)-2-methylphenyl)-2-(dimethylamino)acetamide (3j).** Yield: 51%, mp: 215–216 °C, 1H NMR (400 MHz, DMSO-d6) $\delta$ 9.18 (s, 1H), 9.13 (s, 1H), 9.05 (s, 1H), 8.08 (d, $J$ = 3.6 Hz, 1H), 7.55 (s, 1H), 7.39–7.45 (m, 1H), 7.27 (dd, $J$ = 8.4 Hz, 2.4 Hz, 1H), 7.21 (t, $J$ = 8.0 Hz, 2H), 6.82 (d, $J$ = 8.4 Hz, 1H), 3.03 (s, 2H), 2.30 (s, 6H), 2.06 (s, 3H); $^{13}$C NMR (100 MHz, $CDCl_3$) $\delta$ 168.3, 158.3 (dd, $J_{C-F}$ = 249 Hz, 5 Hz, 2C), 155.6 (d, $J_{C-F}$ = 3 Hz), 150.4 (d, $J_{C-F}$ = 11 Hz), 141.5 (d, $J_{C-F}$ = 245 Hz), 141.1 (d, $J_{C-F}$ = 19 Hz), 138.5, 135.7, 130.3, 127.3 (t, $J_{C-F}$ = 10 Hz), 120.9, 114.7, 114.5 (t, $J_{C-F}$ = 16 Hz), 111.7 (dd, $J_{C-F}$ = 18 Hz, 5 Hz, 2C), 111.7, 63.7, 46.0 (2C), 16.9; HR-ESI-MS: $m/z$ = 431.1786 $[M + H]^+$, calcd for $C_{21}H_{22}F_3N_6O$: 431.1802.

***N*-(4-((4-((2,6-Difluorophenyl)amino)-5-fluoropyrimidin-2-yl)-amino)phenyl)-2-(dimethylamino)acetamide (3k).** Yield: 74%, mp: 225–227 °C, 1H NMR (400 MHz, $CDCl_3$) $\delta$ 8.97 (s, 1H), 7.97 (d, $J$ = 2.8 Hz, 1H), 7.38 (d, $J$ = 8.8 Hz, 2H), 7.33 (d, $J$ = 8.8 Hz, 2H), 7.27–7.29 (m, 1H), 7.03 (t, $J$ = 8.4 Hz, 2H), 6.88 (s, 1H), 6.31 (s, 1H), 3.07 (s, 2H), 2.38 (s, 6H); $^{13}$C NMR (100 MHz, $CDCl_3$) $\delta$ 168.5, 158.5 (dd, $J_{C-F}$ = 249 Hz, 4 Hz, 2C), 155.7 (d, $J_{C-F}$ = 3 Hz), 150.6 (d, $J_{C-F}$ = 12 Hz), 141.5 (d, $J_{C-F}$ = 246 Hz), 141.3 (d, $J_{C-F}$ = 20 Hz), 136.2, 132.1, 127.6 (t, $J_{C-F}$ = 10 Hz), 120.0 (2C), 119.1 (2C), 114.5 (t, $J_{C-F}$ = 16 Hz), 111.9 (dd, $J_{C-F}$ = 18 Hz, 5 Hz, 2C), 63.7, 46.1 (2C); HR-ESI-MS: $m/z$ = 417.1629 $[M + H]^+$, calcd for $C_{20}H_{20}F_3N_6O$: 417.1645.

***N*-(2-((4-((2,6-Difluorophenyl)amino)-5-fluoropyrimidin-2-yl)-amino)phenyl)-2-(dimethylamino)acetamide (3l).** Yield: 28%, mp: 192–193 °C, $^1$H NMR (400 MHz, $CDCl_3$) $\delta$ 9.44 (s, 1H), 7.94 (d, $J$ = 2.4 Hz, 1H), 7.69 (d, $J$ = 7.6 Hz, 1H), 7.43 (d, $J$ = 7.6 Hz, 1H), 7.18–7.23 (m, 1H), 7.12 (t, $J$ = 7.6 Hz, 1H), 7.09 (t, $J$ = 7.6 Hz, 1H), 6.95 (t, $J$ = 8.0 Hz, 2H), 6.87 (s, 1H), 6.27 (s, 1H), 3.07 (s, 2H), 2.27 (s, 6H); $^{13}$C NMR (100 MHz, $CDCl_3$) $\delta$ 169.2, 158.2 (dd, $J_{C-F}$ = 248 Hz, 4 Hz, 2C), 156.5 (d, $J_{C-F}$ = 3 Hz), 150.7 (d, $J_{C-F}$ = 11 Hz), 141.7 (d, $J_{C-F}$ = 245 Hz), 141.2 (d, $J_{C-F}$ = 19 Hz), 131.3, 131.2, 127.4 (t, $J_{C-F}$ = 10 Hz), 125.4, 125.3, 124.9, 123.7, 114.1 (t, $J_{C-F}$ = 16 Hz), 111.7 (dd, $J_{C-F}$ = 18 Hz, 5 Hz, 2C), 63.2, 45.7 (2C); HR-ESI-MS: $m/z$ = 417.1635 $[M + H]^+$, calcd for $C_{20}H_{20}F_3N_6O$: 417.1645.

 

### General procedure for the preparation of (16)

Compound **14m** (1.08 g, 5 mmol), morpholine (1.31 g, 15 mmol), BINAP (150 mg, 0.24 mmol), $Pd(OAc)_2$ (50 mg, 0.22 mmol), and $Cs_2CO_3$ (3.25 g, 10 mmol) were added to toluene(10 mL). Nitrogen was bubbled through the reaction mixture for 5 min, and then the mixture was heated to 120 °C under atmosphere for 8 h. The mixture was filtered and the filtrate was concentrated under vacuum. The crude product was purified by column chromatography on flash silica gel, and eluted with petroleum ether/ethyl acetate (50 : 1) to afford compound **15m** as a yellow solid (800 mg, 72%).

Compound **15m** (260 mg, 1.17 mmol) was dissolved in the mixture of methanol and ethyl acetate, Pd/C (10% Pd, 26 mg) was then added. The mixture was stirred under hydrogen atmosphere for 4 h at room temperature. Pd/C was filtered by diatomite and the solvents were removed under reduced pressure to afford compound **16m** as a gray solid (200 mg, 89%).

Compounds **16n** and **16o** were prepared from other starting materials with the same procedure as described for **16m**.

### General procedure for the preparation of (3m–3o)

Compound **16m** (134 mg, 0.7 mmol), **8e** (181 mg, 0.7 mmol), X-phos (33 mg, 0.07 mmol), $Pd_2(dba)_3$ (32 mg, 0.035 mmol), and $K_2CO_3$ (290 mg, 2.1 mmol) were added to toluene (1 mL) and tertiary butanol (1 mL). Nitrogen was bubbled through the reaction mixture for 5 min, and then the reaction vessel was sealed and heated under microwave irradiation to 125 °C for 25 min. The mixture was filtered and the filtrate was concentrated under vacuum. After concentration, the crude product purified by column chromatography on flash silica gel, eluted with DCM/MeOH (80 : 1) to afford compound **3m** as a white solid (150 mg, 51%).

Compounds **3n** and **3o** were prepared from **16n** and **16o** respectively with the same procedure as described for **3m**.

***N*⁴-(2,6-Difluorophenyl)-5-fluoro-*N*²-(3-(4-methylpiperazin-1-yl)-phenyl) pyrimidine-2,4-diamine (3m).** Yield: 51%, mp: 170–172 °C, $^1$H NMR (400 MHz, DMSO-d6) $\delta$ 9.18 (s, 1H), 8.87 (s, 1H), 8.09 (d, $J$ = 3.2 Hz, 1H), 7.37–7.44 (m, 1H), 7.21 (t, $J$ = 8.0 Hz, 2H), 7.02 (d, $J$ = 8.0 Hz, 1H), 6.96 (s, 1H), 6.83 (t, $J$ = 8.0 Hz, 1H), 6.40 (d, $J$ = 8.4 Hz, 1H), 2.95 (s, 4H), 2.39 (s, 4H), 2.20 (s, 3H); $^{13}$C NMR (125 MHz, $CDCl_3$) $\delta$ 158.6 (dd, $J_{C-F}$ = 250 Hz, 5 Hz, 2C), 155.9 (d, $J_{C-F}$ = 4 Hz), 152.0, 150.7 (d, $J_{C-F}$ = 11 Hz), 141.8 (d, $J_{C-F}$ = 245 Hz), 141.2 (d, $J_{C-F}$ = 20 Hz), 140.8, 129.4, 127.5 (t, $J_{C-F}$ = 10 Hz), 114.7 (t, $J_{C-F}$ = 15 Hz), 112.0 (dd, $J$ = 20 Hz, 5 Hz, 2C), 110.6, 110.3, 106.7, 55.3 (2C), 49.2 (2C), 46.3; HR-ESI-MS: $m/z$ = 415.1842 $[M + H]^+$, calcd for $C_{21}H_{22}F_3N_6$: 415.1853.

***N*⁴-(2,6-Difluorophenyl)-5-fluoro-*N*²-(3-(4-methyl-1,4-diazepan-1-yl)phenyl) pyrimidine-2,4-diamine (3n).** Yield: 34%, mp: 101–103 °C, $^1$H NMR (400 MHz, $CDCl_3$) $\delta$ 7.98 (d, $J$ = 2.8 Hz, 1H), 7.21–7.29 (m, 1H), 7.01 (t, $J$ = 8.4 Hz, 3H), 6.83 (d, $J$ = 8.0 Hz, 1H), 6.74 (s, 1H), 6.68 (s, 1H), 6.31 (dd, $J$ = 8.0 Hz, 1.6 Hz, 1H), 6.22 (s, 1H), 3.49 (t, $J$ = 4.4 Hz, 2H), 3.39 (t, $J$ = 6.4 Hz, 2H), 2.65 (t, $J$ = 4.4 Hz, 2H), 2.53 ($J$ = 4.4 Hz, 2H), 2.36 (s, 3H), 1.94–2.00 (m, 2H); $^{13}$C NMR (100 MHz, $CDCl_3$) $\delta$ 157.3 (dd, $J_{C-F}$ = 249 Hz, 5 Hz, 2C), 154.8 (d, $J_{C-F}$ = 3 Hz), 149.4 (d, $J_{C-F}$ = 11 Hz), 148.7, 140.4 (d, $J_{C-F}$ = 245 Hz), 140.0 (d, $J_{C-F}$ = 19 Hz), 139.7, 128.3, 126.3 (t, $J_{C-F}$ = 10 Hz), 113.4 (t, $J_{C-F}$ = 16 Hz), 110.7 (dd, $J_{C-F}$ = 18 Hz, 5 Hz, 2C), 105.8, 104.9, 101.1, 57.1, 56.0, 47.5, 47.2, 45.6, 26.7; HR-ESI-MS: $m/z$ = 429.2005 $[M + H]^+$, calcd for $C_{22}H_{24}F_3N_6$: 429.2009.

***N*⁴-(2,6-difluorophenyl)-5-fluoro-*N*²-(4-methyl-3-morpholino-phenyl)pyrimidine-2,4-diamine (3o).** Yield: 47%, mp: 173–175 °C, $^1$H NMR (400 MHz, $CDCl_3$) $\delta$ 7.97 (d, $J$ = 2.8 Hz, 1H), 7.25–7.32 (m, 1H), 7.11 (d, $J$ = 8.0 Hz, 1H), 7.00–7.05 (m, 3H), 6.97 (d, $J$ = 8.0 Hz, 2H), 6.29 (s, 1H), 3.81 (t, $J$ = 4.4 Hz, 4H), 2.78 (t, $J$ = 4.4 Hz, 4H), 2.22 (s, 3H); $^{13}$C NMR (125 MHz, $CDCl_3$) $\delta$ 158.5 (dd, $J_{C-F}$ = 250 Hz, 4 Hz, 2C), 155.9 (d, $J_{C-F}$ = 3 Hz), 151.6, 150.7 (d, $J_{C-F}$ = 10 Hz), 141.6 (d, $J_{C-F}$ = 245 Hz), 141.1 (d, $J_{C-F}$ = 19 Hz), 138.5, 131.2, 127.6 (t, $J_{C-F}$ = 10 Hz), 126.2, 114.6 (t, $J_{C-F}$ = 16 Hz), 114.1, 111.9 (dd, $J_{C-F}$ = 19 Hz, 4 Hz, 2C), 110.1, 67.5 (2C), 52.1 (2C), 17.3; HR-ESI-MS: $m/z$ = 416.1683 $[M + H]^+$, calcd for $C_{21}H_{21}F_3N_5O$: 416.1693.

### Kinase assays

The enzymatic assays against CDK2/cyclin A and CDK9/cyclin T1 were performed by following experimental protocols published previously. The assays were completed through contract services provided by Cerep Drug Discovery Services Co. Ltd.

### CDK2/cyclin A kinase assay

The kinase assay against CDK2/cyclin A was performed by following experimental protocols described in the ref. 23 The compounds were mixed with the enzyme (2.28 ng) in a buffer containing 40 mM Hepes/Tris(pH 7.4), 0.8 mM EGTA/Tris, 8 mM $MgCl_2$, 1.6 mM DTT and 0.008% Tween 20. Thereafter, the reaction was initiated by adding 100 nM of the substrate Ulight-CFFKNIVTPRTPPPSQGK-amide (MBP) and 10 μM ATP, and the mixture was incubated for 15 minutes at room temperature. For the control basal measurements, the enzyme was omitted from the reaction mixture. Following incubation, the reaction was stopped by adding 13 mM EDTA. After 5 minutes, the anti-phospho-MBP antibody labeled with europium chelate was added. After 60 more minutes, the fluorescence transfer was measured at $\lambda_{ex}$ = 337 nm, $\lambda_{em}$ = 620 nm and $\lambda_{em}$ = 665 nm using a microplate reader (Envision, Perkin Elmer). The enzyme activity was determined by dividing the signal measured at 665 nm by that measured at 620 nm (ratio). The results were expressed as a percent inhibition of the control enzyme activity. The compounds were tested in each experiment at six concentrations to obtain an inhibition curve from which the $IC_{50}$ values were calculated.

### CDK9/cyclin T1 kinase assay

The kinase assay against CDK9/cyclin T1 was performed by following experimental protocols described in the ref. 24 The compounds were mixed with the enzyme (21.72 ng) in a buffer containing 40 mM Hepes/Tris(pH 7.4), 0.8 mM EGTA/Tris, 8 mM $MgCl_2$, 1.6 mM DTT and 0.008% Tween 20. Thereafter, the reaction was initiated by adding 100 nM of the substrate Ulight-CFFKNIVTPRTPPPSQGK-amide (MBP) and 10 μM ATP, and the mixture was incubated for 90 minutes at room temperature. For control basal measurements, the enzyme was omitted from the reaction mixture. Following incubation, the

reaction was stopped by adding 13 mM EDTA. After 5 minutes, the anti-phospho-MBP antibody labeled with europium chelate was added. After 60 more minutes, the fluorescence transfer was measured at $\lambda_{ex} = 337$ nm, $\lambda_{em} = 620$ nm and $\lambda_{em} = 665$ nm using a microplate reader (Envision, Perkin Elmer). The enzyme activity was determined by dividing the signal measured at 665 nm by that measured at 620 nm (ratio). The results were expressed as a percent inhibition of the control enzyme activity. The compounds were tested in each experiment at six concentrations to obtain an inhibition curve from which the $IC_{50}$ values were calculated.

### SRB assay

The following five human tumor cell lines were used in the assay: MDA-MB-231 (human breast carcinoma cell line), MCF-7 (Michigan Cancer Foundation-7), A549 (lung cancer), KB (nasopharyngeal carcinoma) and KB-vin (vincristine-resistant KB subline). All cell lines were obtained from the Lineberger Comprehensive Cancer Center (UNC-CH) or from ATCC (Rockville, MD) and were cultured in RPMI-1640 medium supplemented with 25 mM HEPES, 0.25% sodium bicarbonate (Gibco), 10% fetal bovine serum (Corning), and 100 μg $mL^{-1}$ streptomycin, 100 IU $mL^{-1}$ penicillin, and 0.25 μg $mL^{-1}$ amphotericin B (Corning).

The cytotoxicity assay was performed by following experimental protocols described in the ref. 25 Freshly trypsinized cell suspensions were seeded in 96-well microtiter plates at densities of 4000–11 000 cells per well with compounds added from DMSO-diluted stock. After 3 days in culture, attached cells were fixed in cold 10% trichloroacetic acid and then stained with 0.04% sulforhodamine B (SRB). The absorbance at 515 nm was measured using a microplate reader (ELx800, BioTek) operated by Gen5 software (BioTek) after solubilizing the bound dye with 10 mM Tris. The mean $IC_{50}$ is the concentration of agents that reduces cell growth by 50% under the experimental conditions and it is the average from three independent determinations.

### Cell cycle analysis

The flow cytometry was performed by following protocols described previously.[18] Briefly, MDA-MB-231 cells were treated for 24 h with compound at the concentration of five-fold of $GI_{50}$. Cells were fixed and stained with propidium iodide (PI) (BD Biosciences) followed by analysis of cell cycle using flow cytometer (LSRFortessa, BD Biosciences).

### Molecular modeling

The structure of compound **3g** was generated and molecular docking was performed with the Discovery Studio 2017 software package (Accelrys, San Diego, USA). Due to the structural similarity between compound **3g** and the inhibitor co-crystalized, the 3D structures of CDK2 (4BCP) and CDK9 (4BCG) were selected and obtained from the Protein Data Bank for docking study. The docking calculation was carried out with the CDOCKER protocol. In the process of CDOCKER docking, the pose cluster radius was set to "0.5". Other parameters were used as default.

## Conclusion

In conclusion, twenty-four $N^2$,$N^4$-disubstituted pyrimidine-2,4-diamines derivatives were synthesized and their structure–activity relationship was investigated. Most of the compounds demonstrated potent inhibition against both CDK9 and CDK2. Compounds **3g** and **3c** were identified as the most potent CDK2 and CDK9 inhibitors, and showed $IC_{50}$ values of 83 nM and 65 nM respectively. Furthermore, most compounds showed significant inhibition against tumor cells, including the triple-negative breast cancer cell line MDA-MB-231. These compounds also imposed obvious effects on cell cycle progression in MDA-MB-231 cells, and induced cell cycle arrest in G2/M phase. Preliminary SAR analysis and molecular docking of **3g** provided new clues for further structural optimization of this compound class.

## Conflicts of interest

The authors have no conflicts of interest to declare.

## Acknowledgements

We gratefully acknowledge the financial support from National Natural Science Foundation of China (81172985 and 81261120391) and CAMS Innovation Fund for Medical Sciences (CIFMS, 2016-I2M-3-009) awarded to Z Xiao. Partial support was also supplied from NIH grant CA177584 awarded to K. H. Lee.

## Notes and references

1 M. Malumbres, E. Harlow, T. Hunt, T. Hunter, J. M. Lahti, G. Manning, D. O. Morgan, L.-H. Tsai and D. J. Wolgemuth, *Nat. Cell Biol.*, 2009, **11**, 1275–1276.
2 S. Lim and P. Kaldis, *Development*, 2013, **140**, 3079–3093.
3 A. Marais, Z. Ji, E. S. Child, E. Krause, D. J. Mann and A. D. Sharrocks, *J. Biol. Chem.*, 2010, **285**, 35728–35739.
4 Y.-J. Chen, C. Dominguez-Brauer, Z. Wang, J. M. Asara, R. H. Costa, A. L. Tyner, L. F. Lau and P. Raychaudhuri, *J. Biol. Chem.*, 2009, **284**, 30695–30707.
5 J. Garriga, S. Bhattacharya, J. Calbo, R. M. Marshall, M. Truongcao, D. S. Haines and X. Grana, *Mol. Cell. Biol.*, 2003, **23**, 5165–5173.
6 J. Garriga and X. Graña, *Gene*, 2004, **337**, 15–23.
7 D. H. Price, *Mol. Cell. Biol.*, 2000, **20**, 2629–2634.
8 J. Cicenas and M. Valius, *J. Cancer Res. Clin. Oncol.*, 2011, **137**, 1409–1418.
9 C. Di Giovanni, E. Novellino, A. Chilin, A. Lavecchia and G. Marzaro, *Expert Opin. Invest. Drugs*, 2016, **25**, 1215–1230.
10 V. Malínková, J. Vylíčil and V. Kryštof, *Expert Opin. Ther. Pat.*, 2014, **25**, 1–18.
11 U. Asghar, A. K. Witkiewicz, N. C. Turner and E. S. Knudsen, *Nat. Rev. Drug Discovery*, 2015, **14**, 130–146.
12 Thomson Reuters Integrity, https://integrity.thomsonpharma.com/integrity/xmlxsl/pk_home.util_home, accessed Janaury 2018.

 

13 S. L. Sammons, D. L. Topping and K. L. Blackwell, *Curr. Cancer Drug Targets*, 2017, **17**, 637–649.
14 C. C. O'Sullivan, *Expert Opin. Pharmacother.*, 2016, **17**, 1657–1667.
15 C. Fang, Z. Xiao and Z. Guo, *J. Mol. Graphics Modell.*, 2011, **29**, 800–808.
16 J. Gao, C. Fang, Z. Xiao, L. Huang, C. H. Chen, L. T. Wang and K. H. Lee, *MedChemComm*, 2014, **6**, 444–454.
17 H. Galons, N. Oumata, O. Gloulou and L. Meijer, *Expert Opin. Ther. Pat.*, 2013, **23**, 945–963.
18 K. Nakagawagoto, A. Oda, E. Hamel, E. Ohkoshi, K. H. Lee and M. Goto, *J. Med. Chem.*, 2015, **58**, 2378–2389.
19 L. T. Vassilev, C. Tovar, S. Chen, D. Knezevic, X. Zhao, H. Sun, D. C. Heimbrook and L. Chen, *Proc. Natl. Acad. Sci. U. S. A.*, 2006, **103**, 10660–10665.
20 I. Aliagasmartin, B. Dan, L. Corson, J. Dotson, J. Drummond, C. Fields, O. W. Huang, T. Hunsaker, T. Kleinheinz and E. Krueger, *J. Med. Chem.*, 2009, **52**, 3300–3307.
21 Y. Wang, G. Zhang, G. Hu, Y. Bu, H. Lei, D. Zuo, M. Han, X. Zhai and P. Gong, *Eur. J. Med. Chem.*, 2016, **123**, 80–89.
22 J. Q. Zhang, Y. J. Luo, Y. S. Xiong, Y. Yu, Z. C. Tu, Z. J. Long, X. J. Lai, H. X. Chen, Y. Luo and J. Weng, *J. Med. Chem.*, 2016, **59**, 7268–7274.
23 L. Meijer, A. Borgne, O. Mulner, J. P. Chong, J. J. Blow, N. Inagaki, M. Inagaki, J. G. Delcros and J. P. Moulinoux, *Eur. J. Biochem.*, 1997, **243**, 527–536.
24 G. De Falco and A. Giordano, *J. Cell. Physiol.*, 1998, **177**, 501–506.
25 M. V. B. Reddy, Y. C. Shen, E. Ohkoshi, K. F. Bastow, K. Qian, K. H. Lee and T. S. Wu, *Eur. J. Med. Chem.*, 2012, **47**, 97–103.